



Advanced Detector Technology

Luciano Musa - CERN



Lecture 3/3
CERN, 2 September 2017

Electromagnetic Calorimetry

Basic principles

Calorimeters – General Considerations

Calorimeters (Electromagnetic and Hadronic Cal)

massive detectors in which particles are completely stopped

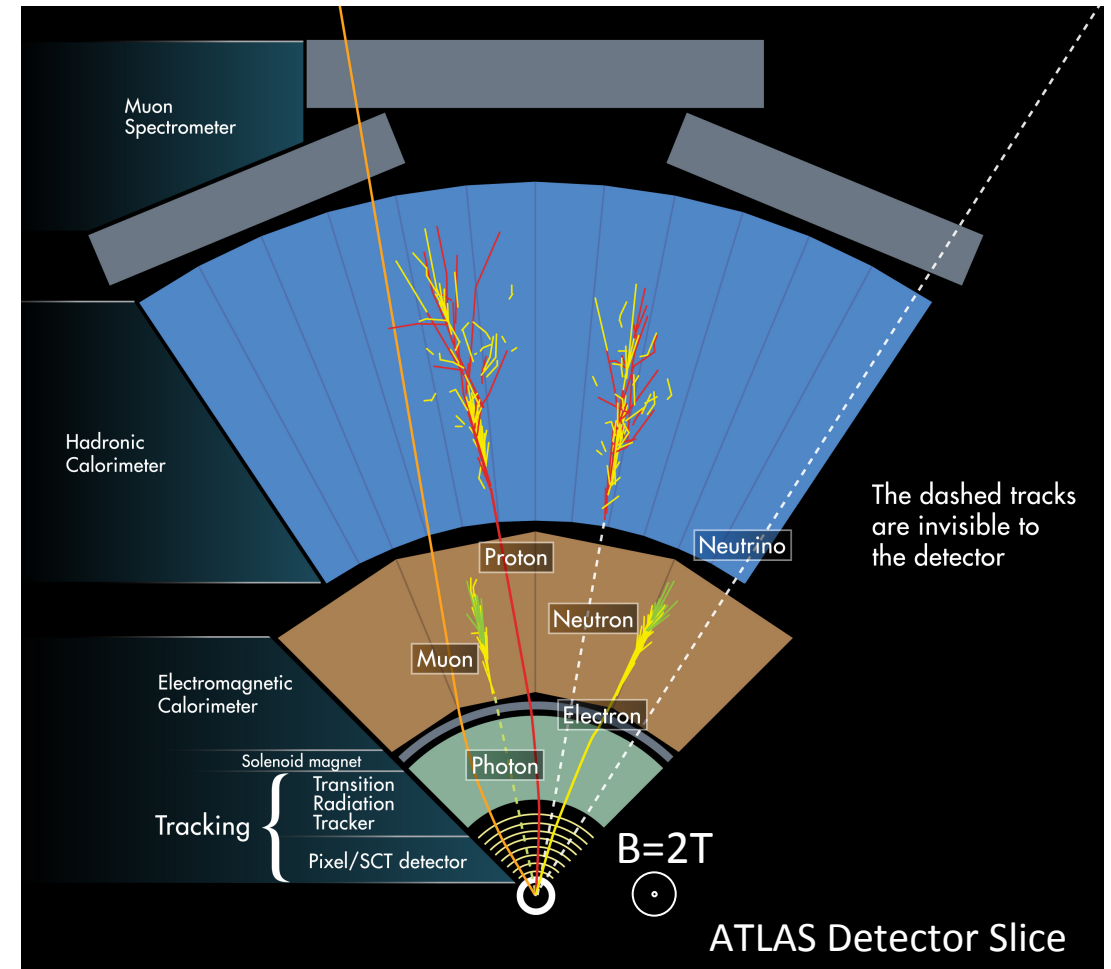
⇒ Calorimetry is a destructive measurement

All particles except muons and neutrinos deposit all energy in the calorimeter by production electromagnetic and/or hadronic showers

γ , e^\pm : deposit all energy in the EM Calorimeter

- showers are indistinguishable, but e^\pm can be identified by the presence of a track in the tracking system

Hadrons: deposit most of their energy in the Hadr Cal (part of it in the EM Cal) individual members of the families of charged and neutral hadrons cannot be distinguished in a calorimeter



Calorimeters are usually segmented and instrumented such to provide the particle's 4-vector

Calorimeters – General Considerations

Measurement resolution: energy vs. momentum

$$\text{Magnetic Spectrometer: } \frac{\sigma_p}{p} \propto p$$

$$\text{Calorimeter}^{(*)}: \frac{\sigma_E}{E} \propto \frac{1}{\sqrt{E}} \quad (*) \text{most cases}$$

Calorimeter energy resolution
improves with energy



calorimeters are well suited for
very high energy experiments

Energy Flow (total & missing)

e.g. provide indirect detection of neutrinos and their energy by a measurement of the event missing energy

Shower direction - shower position and direction used to identify different particles

e.g. to distinguish e and γ from π and μ on the basis of their different interactions with the detector

Fast information - measure the arrival time of particles and are also commonly used for trigger purposes

They can provide fast signals that easy to process and interpret

Calorimeters – General Considerations

Calorimeters are space effective

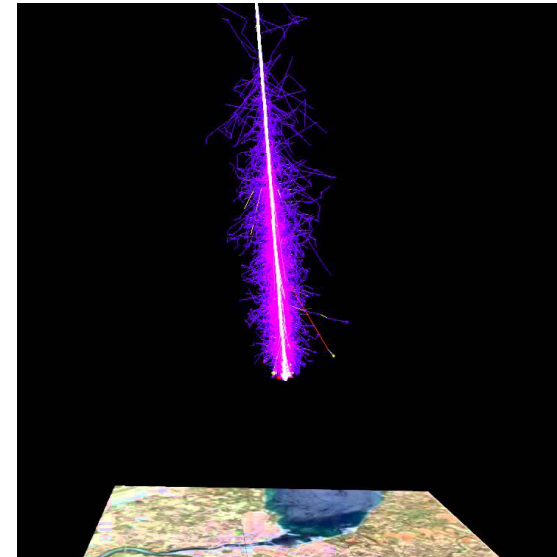
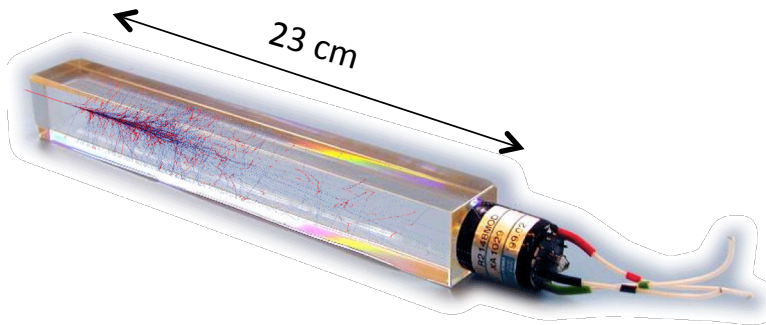
$$\text{Magnetic Spectrometer: } \frac{\sigma_p}{p} \propto \frac{p}{BL^2}$$

BL^2 must increase linearly with p to keep resolution constant

$$\text{Calorimeter shower length: } L \propto \ln \frac{E}{E_0}$$

Detector thickness grows only logarithmically with the energy of the particle

Can be made rather compact, even at the LHC energy scale



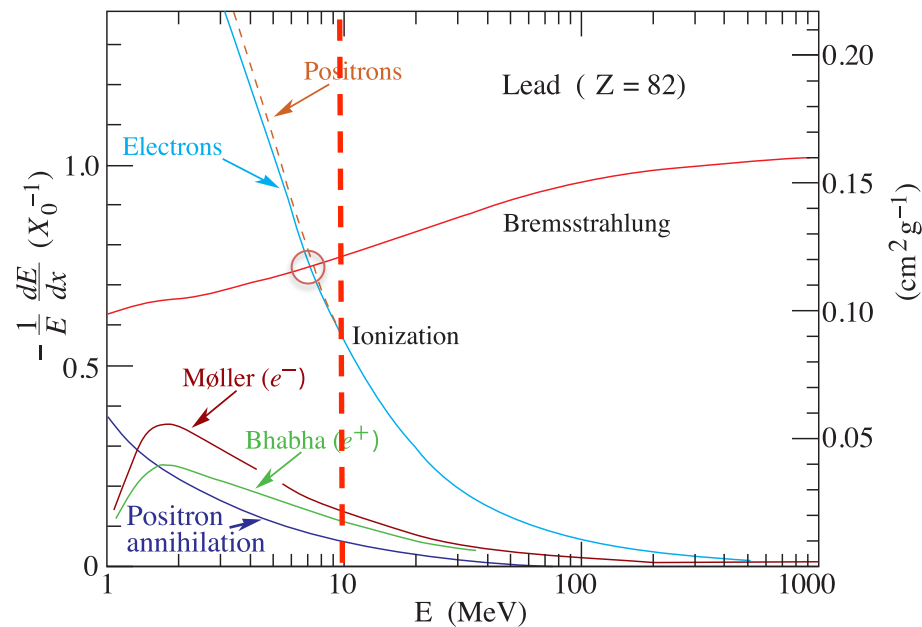
(NOT at the EeV scale)

Simulation of a 1EeV (10^{18} eV) proton cosmic air shower

Physics of electromagnetic cascade

At low energies

- Electrons lose their energy mainly through collisions with the atoms and molecules of the material: ionization and thermal excitation.
- Photons lose their energy through Compton scattering and photoelectric effect



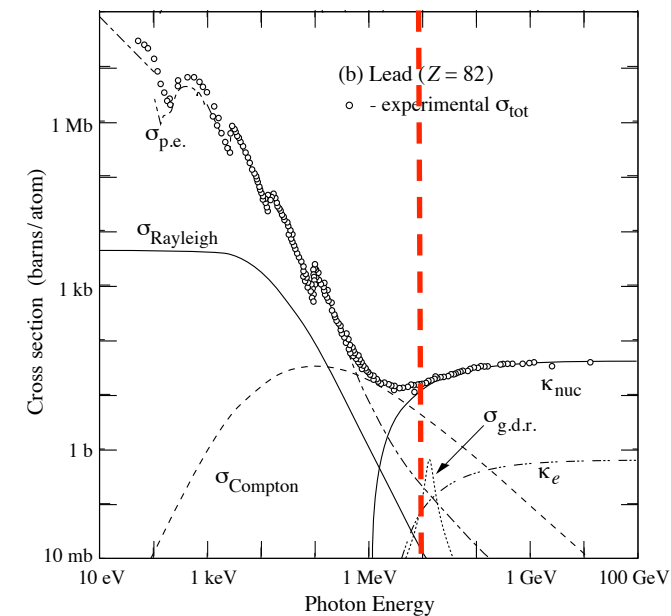
Fractional energy loss per radiation length in lead as a function of electron or positron energy

For $E > \sim 10$ MeV

- Electron energy loss mostly by bremsstrahlung
- Photon interactions mainly produce e^-e^+ pairs

For $E > 1$ GeV

- Both processes become roughly energy independent



Photon total cross-section as function of energy in lead. Contribution of different processes

Physics of electromagnetic cascade

Electrons, positrons and photons of sufficiently high energy $E \geq 1\text{GeV}$ incident on a block of material produce

⇒ Secondary photons by bremsstrahlung

⇒ Secondary electrons-positrons by pair production

⇒ These secondary particles in turn produce other particles by the same mechanism

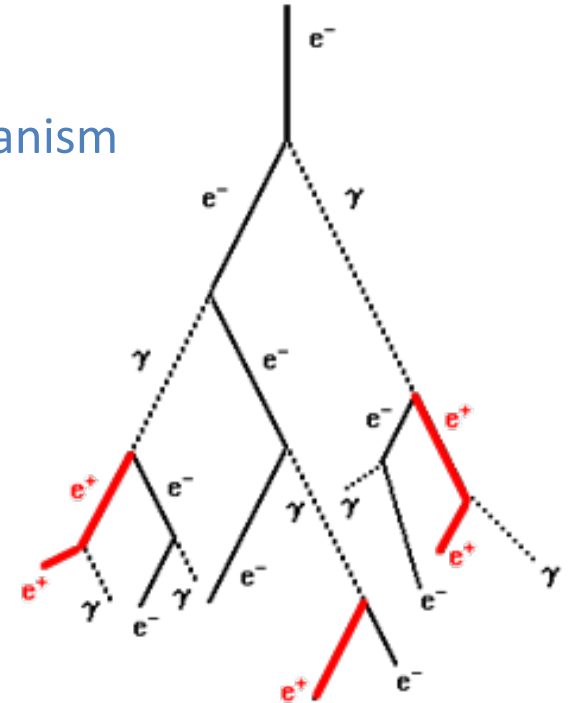


cascade of particles (electromagnetic shower)

Simulation of electromagnetic shower

$\gamma + \text{nucleus} \rightarrow e^+ + e^- + \text{nucleus}$

$e + \text{nucleus} \rightarrow e^+ + \gamma + \text{nucleus}$



The number of particles in the shower increases until the energy of the electron component falls below a critical energy E_c , where energy is mainly dissipated by ionization and excitation and not in the generation of other particles

Physics of electromagnetic cascade

Main features of an electromagnetic shower

- Number of particles in shower
- Location of shower maximum
- Longitudinal distribution (length)
- Transverse shower distribution (width)

X_0 : it represents the average distance x than an electron needs to travel to reduce its energy to $1/e$ of its original energy E_0

The intensity of a photon beam traversing a block is reduced to $1/e$ of its initial intensity I_0 after travelling a distance $x = 9/7 X_0$

Critical energy E_c : ionization losses = bremsstrahlung losses

Physical scale of a shower similar for e^\pm and γ can be described in terms of one parameter

radiation length X_0

which depends on the characteristics of the material

$$X_0 (g/cm^2) \approx \frac{716 g cm^{-2} A}{Z(Z+1) \ln(287/\sqrt{Z})}$$

$$\langle E(x) \rangle = E_0 e^{\left(-\frac{x}{X_0}\right)}$$

$$\langle I(x) \rangle = I_0 e^{\left(-\frac{7}{9} \frac{x}{X_0}\right)}$$

$$E_c \approx \frac{610}{Z+1.24} MeV \approx \frac{610}{Z} MeV$$

Physics of electromagnetic cascade

$$t_{\max} \approx \ln \frac{E_0}{E_c} + t_0$$

Shower length grows logarithmically with the energy of incident particle



Detector thickness grows logarithmically with particle energy

$t_0 = -0.5$ (+0.5) electrons (photons)

The calorimeter thickness containing 95% of the shower is approximately

$$t_{95\%} \approx t_{\max} + 0.08Z + 9.6$$

$t_{95\%}$ and t_{\max} are measured in units of X_0

In **calorimeters with thickness $t \approx 25X_0$** , the shower longitudinal leakage beyond the end of the active detector is much less than 1% up to incident electron **energies of ~ 300 GeV**.

Even for the CERN LHC energies (~ 1 TeV), electromagnetic calorimeters are very compact devices

ATLAS ECAL (Pb / liquid Ar, $X_0 \approx 1.8$ cm): thickness ≈ 45 cm ($25 X_0$)

CMS ECAL (PbWO₄, $X_0 \approx 0.9$ cm): thickness ≈ 23 cm ($25 X_0$)

Physics of electromagnetic cascade

The transverse size of an electromagnetic shower is mainly due to multiple scattering of electrons and positrons away from the shower axis

A measurement of the transverse size, integrated over the shower depth, is given by the Moliere radius (R_M)

$$R_M \left(g/cm^2 \right) \approx 21 MeV \frac{X_0}{E_c \left(MeV \right)}$$

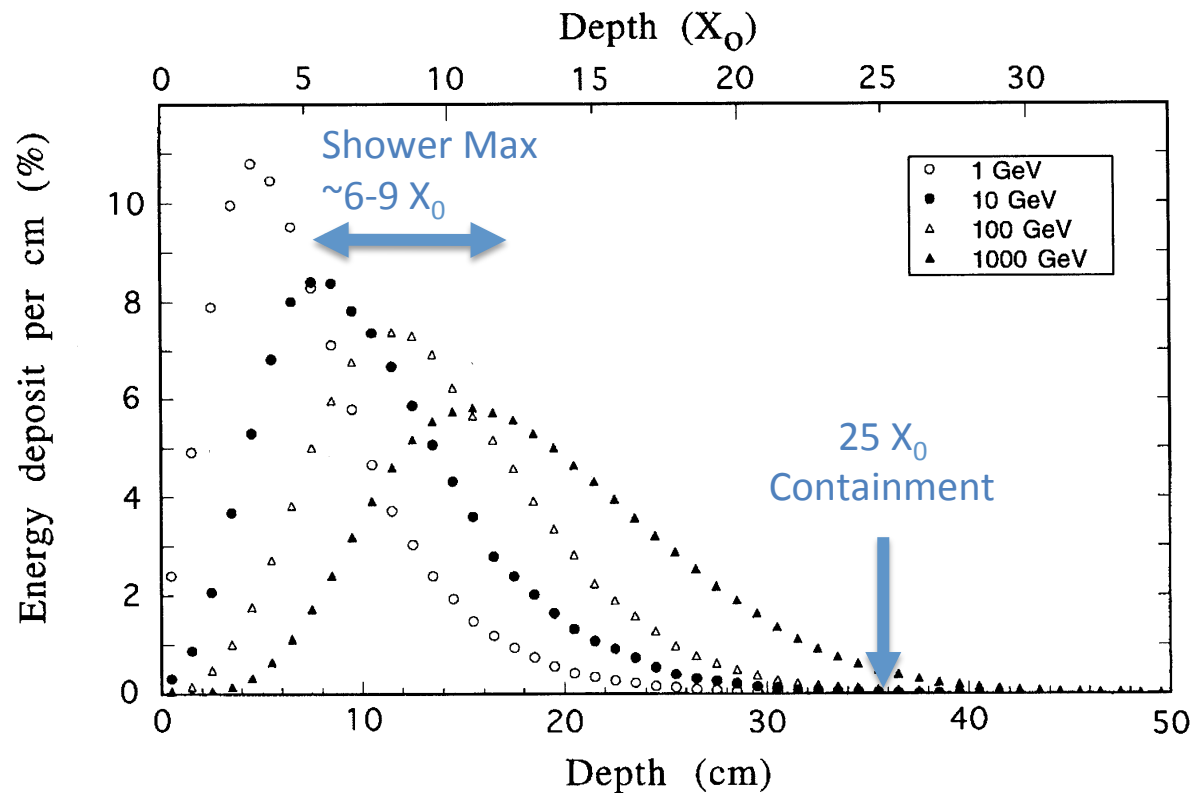
On average, about 90% of the shower energy is contained in a cylinder of radius $\sim 1 R_M$

For most of the calorimeters $R_M \sim$ few centimeters \Rightarrow electromagnetic shower are quite narrow

If a calorimeter is to be used for precision measurements of the shower position

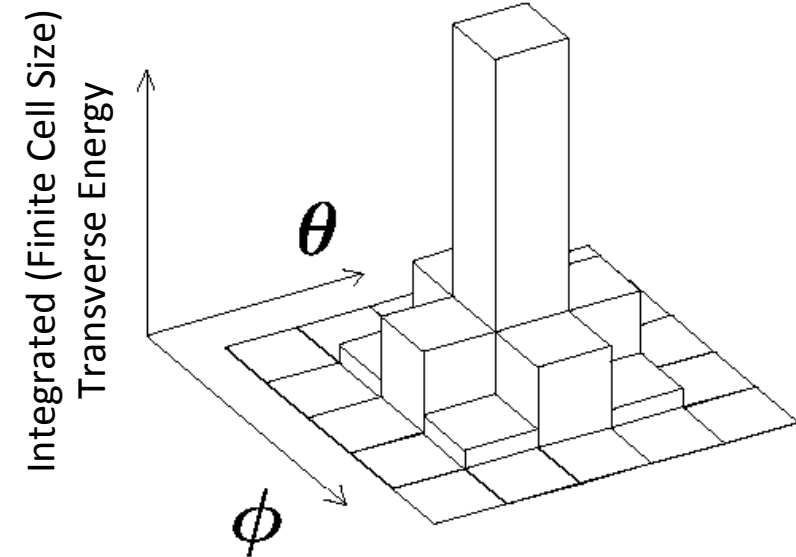
\Rightarrow the cells of a segments calorimeter must be comparable (or smaller) in size to $1 R_M$

EM Shower longitudinal and transverse profile



Longitudinal profile of EM shower in copper
(Courtesy of R. Wigmans)

99% of shower in $3R_M$



Choose Cell Granularity a bit
Smaller than One Moliere Radius

Electromagnetic Calorimeters – Energy Resolution

Ideal calorimeter

- infinite size
- no response deterioration due to instrumental effects (signal collection inefficiency, non uniform response, noise, etc.)

The **intrinsic energy resolution** is mainly due to fluctuations of the total track length of the shower (sum of all ionization tracks of all particles in the shower)

Since the shower development is a stochastic process, the intrinsic energy resolution is from purely statistical arguments

$$\frac{\sigma_E}{E} = \frac{1}{\sqrt{\text{Shower_total_track_length}}} = \frac{1}{\sqrt{E}}$$

The actual energy resolution of a realistic calorimeter is deteriorated by other contributions

$$\frac{\sigma_E}{E} = \frac{a}{\sqrt{E}} \oplus \frac{b}{E} \oplus c$$

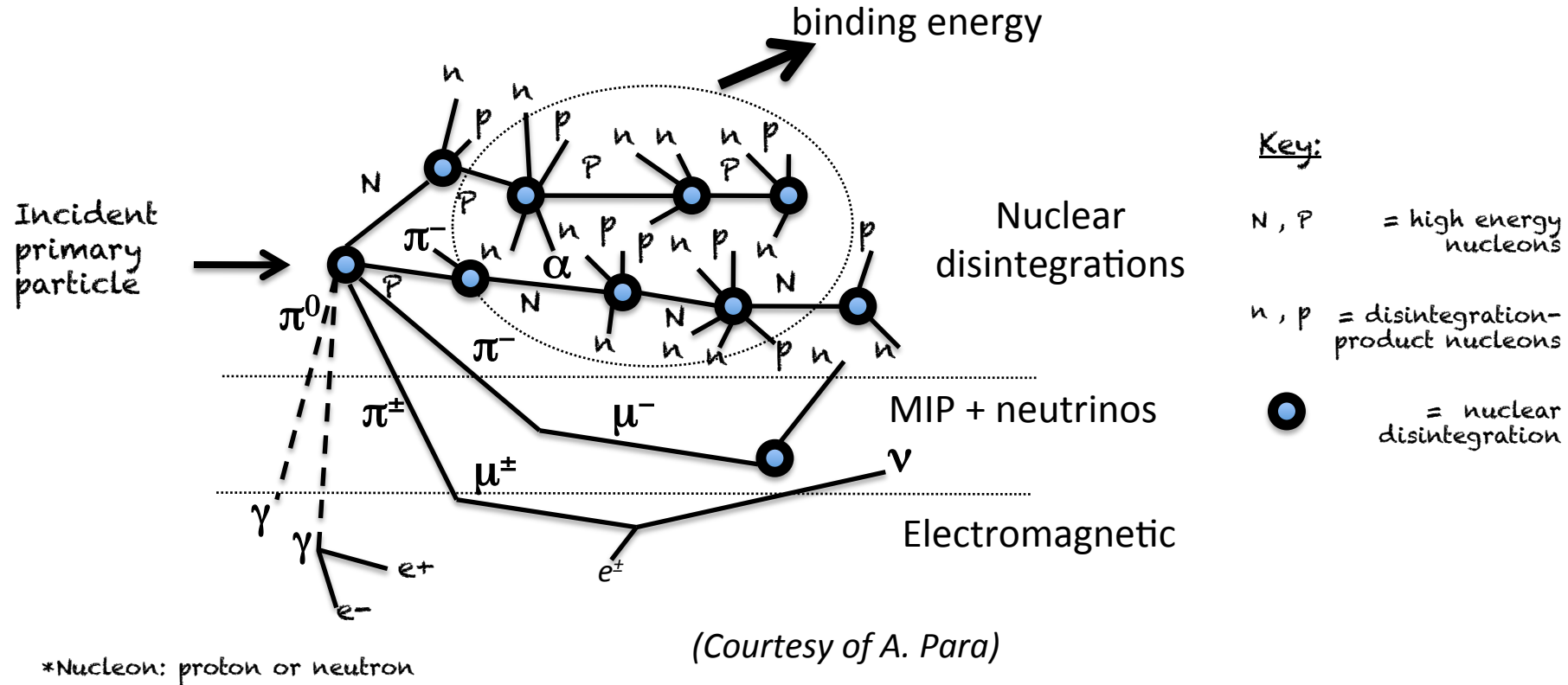
a = stochastic (sampling) term

b = noise term

c = constant term

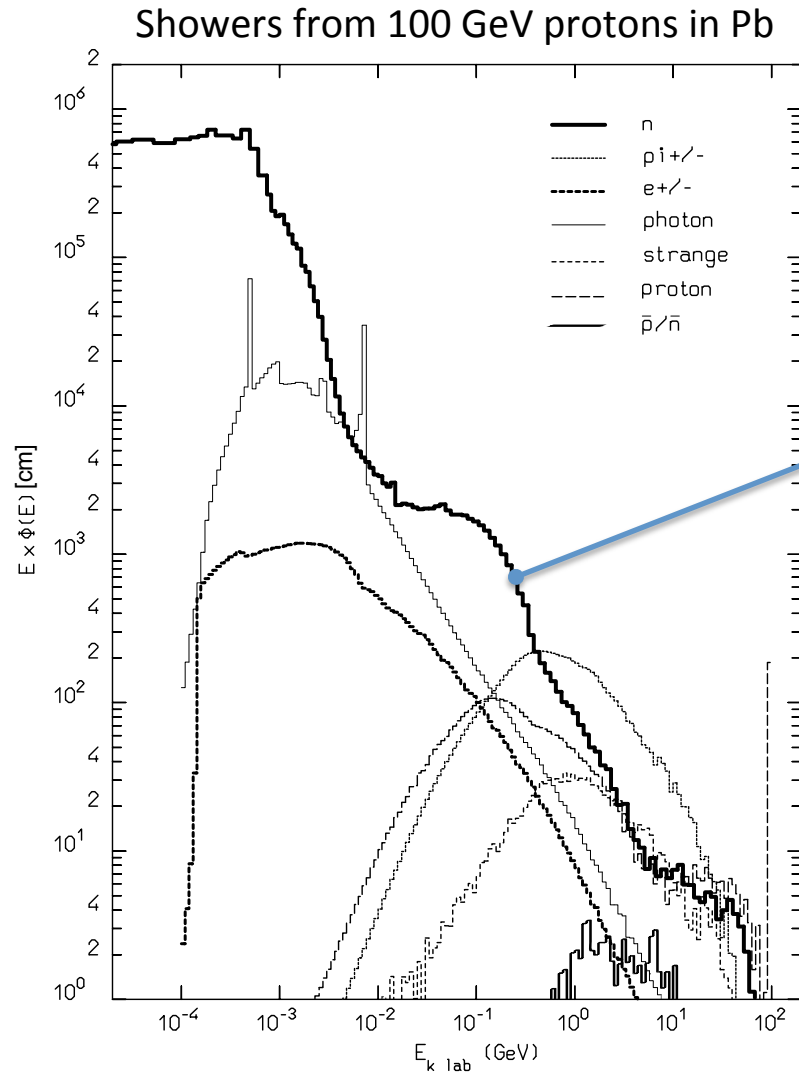
The Physics of Hadronic Showers

The energy degradation of hadrons proceed through an increasing number of (mostly) strong interactions

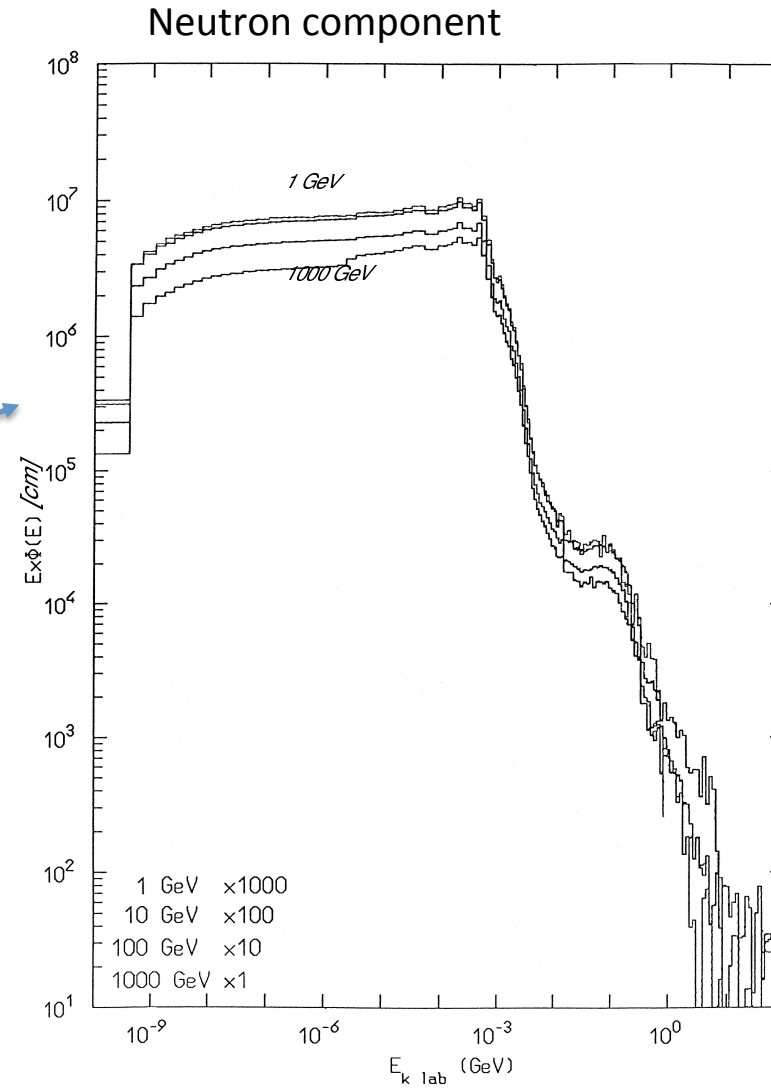


However, complexity of hadronic and nuclear processes produces a multitude of effects that make the HCALs much more complicated instruments to optimize

The Physics of Hadronic Showers



Fluka simulations (Ferrari 2001)



Fluka simulations (Ferrari 2001)

Fast hadronic component

- p,n
- π^\pm, π^0

$$F(\pi^0) = 1/3$$

$\pi^0 \rightarrow \gamma\gamma \Rightarrow$ em shower

“one-way diode”
transfer of energy from
hadronic component to
electromagnetic one

\Rightarrow no further contribution
to hadronic process

The Physics of Hadronic Showers

Nr. of energetic hadronic interactions increases with energy of incident particle



Fraction of electromagnetic cascade will also increase with energy of incident particle

Hadronic fraction $F_h = \left(E/E_0\right)^k \quad k = \ln\alpha / \ln m$

E_0 cutoff energy for further hadronic production (typically $E_0 \approx 1-2$ GeV)

m multiplicity of fast hadrons produced

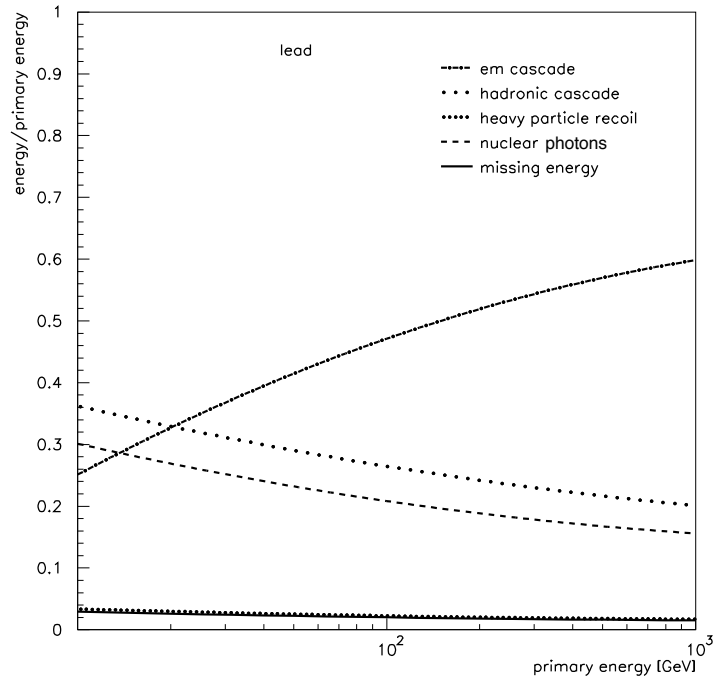
α fraction of hadrons not decaying electromagnetically

$K \approx 0.2$ $F_h \approx 0.5$ for 100 GeV shower
 $F_h \approx 0.3$ for 1 TeV shower

Shower from high energy hadron
dissipates its energy in a flash of photons

The Physics of Hadronic Showers

characteristics components of
proton initiated cascade in Pb



Fluka simulations (Ferrari 2001)

photons from nuclear reaction carry a sizeable fraction of energy

BUT: only a fraction will be recorded in practical calorimeter
(most of these photons are emitted with a considerable delay $\leq 1\mu\text{s}$)

delayed photons, soft neutrons, binding energy,



Nuclear effects produce “invisible energy”

$$E_{\text{vis}}^e = \eta_e E(\text{em})$$

$$E_{\text{vis}}^\pi = \eta_h E(\text{pure hadronic})$$

$\eta_e, \eta_h \dots$ signal efficiencies

$$\frac{E_{\text{vis}}^\pi}{E_{\text{vis}}^e} = 1 - \left(1 - \frac{\eta_h}{\eta_e}\right) F_h$$

in general $\eta_e \neq \eta_h$

Response of hadron calorimeter not linear with energy of incident particle (because F_h decreases with incident energy)

Event-by-event fluctuations in the ratio F_h / F_π will have an impact on the energy resolution

Relative response e/π very important for controlling the performance of an hadronic calorimeter

Calorimeters types

Calorimeters can be generally divided (according to their construction technique) in two main categories

- **Sampling calorimeter**

Consist of **alternating layers** of an **absorber**, a dense material used to degrade the energy of the incident particle, and an **active material** that generates a detectable signal

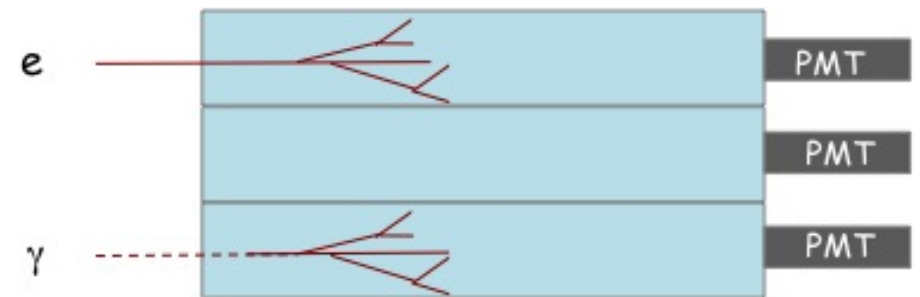
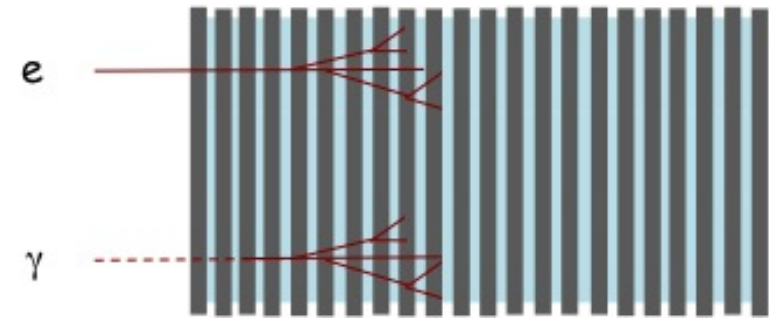
- **Homogenous calorimeters**

Built of **only one type of material** that performs *both energy degradation and signal generation*

Either type is extensively used for ECALs

HCALs are almost exclusively sampling calorimeters

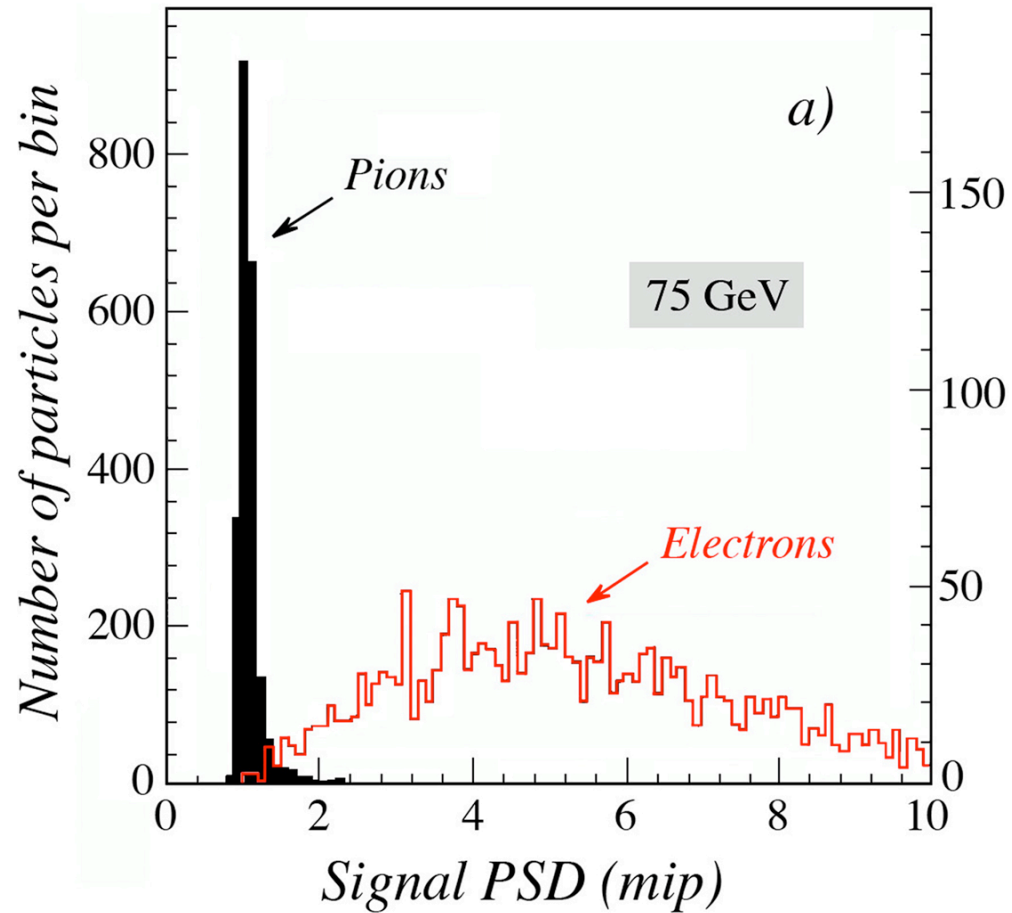
Decision for either depends on application



Note: an homogenous calorimeter could also be segmented longitudinally

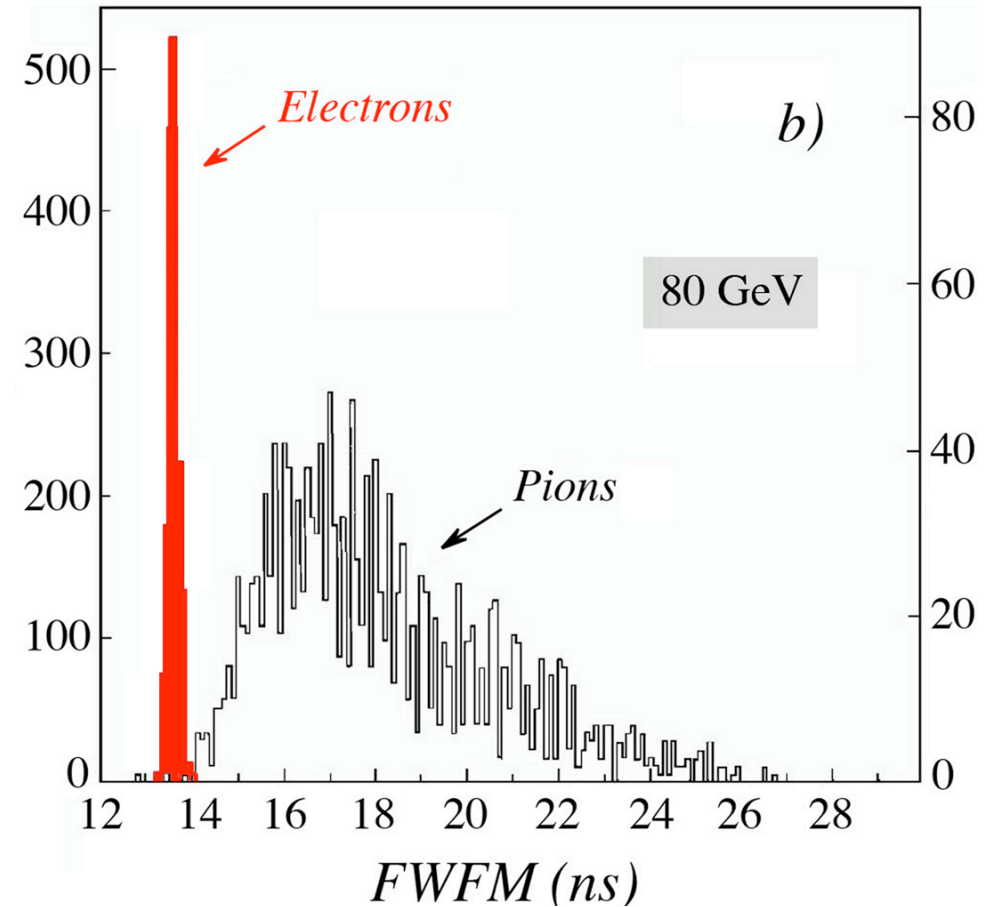
PID with Calorimeters

Using shower profile (pre-shower detector)



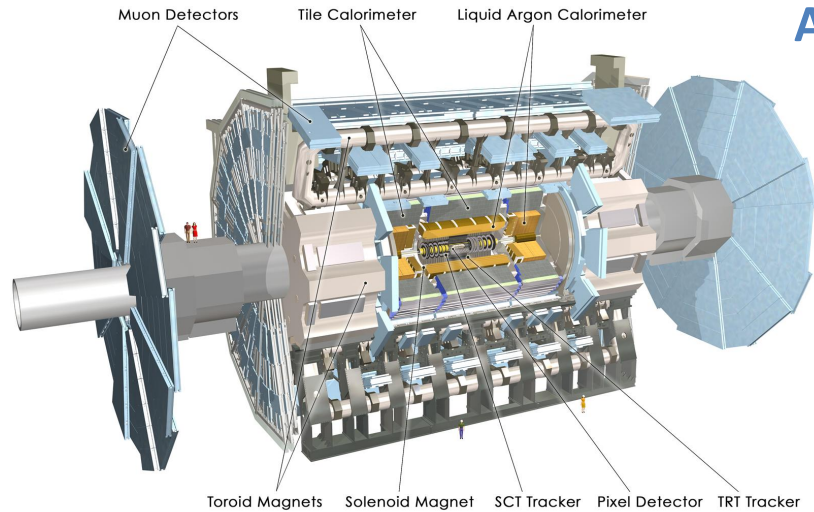
High spatial granularity

Using time structure of the signal

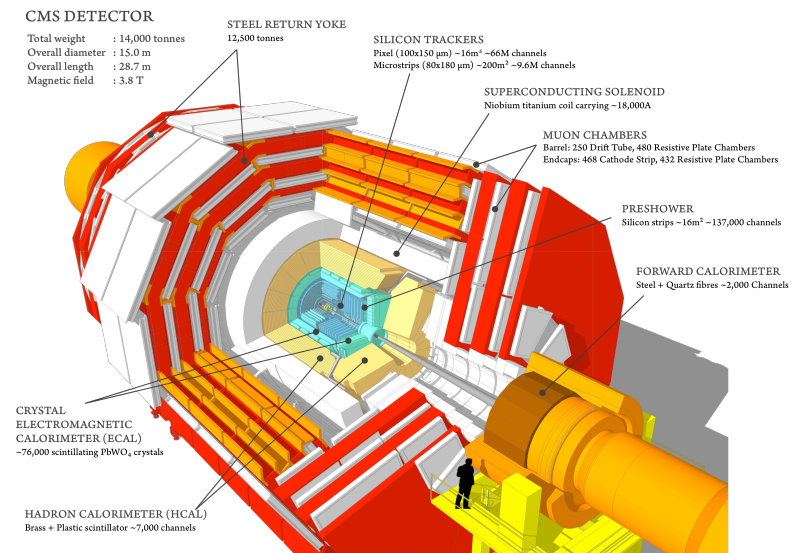


Excellent timing resolution

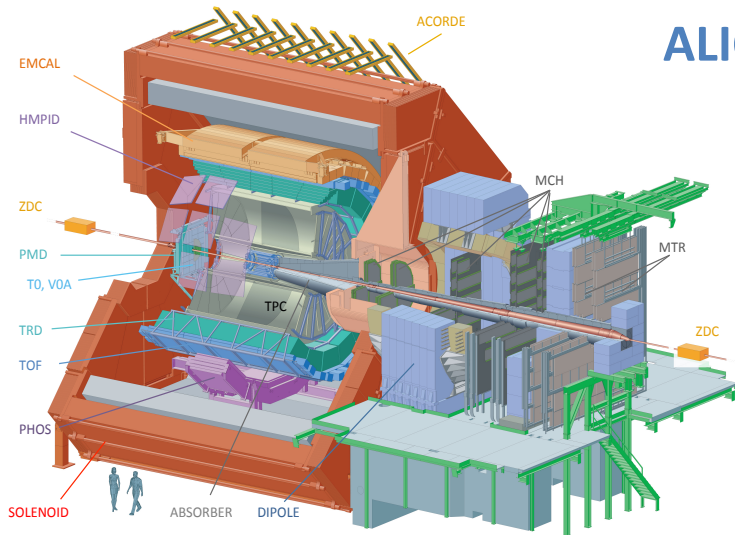
LHC Calorimeters – Lots of Variety



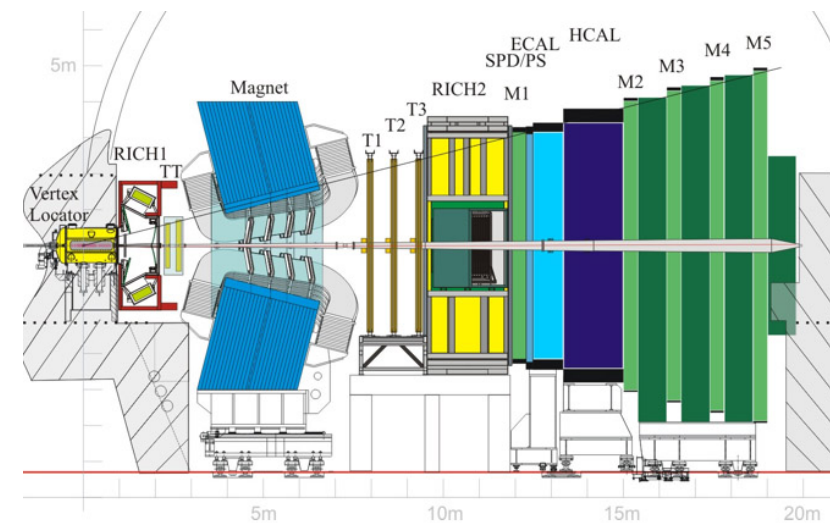
ATLAS



CMS



ALICE



LHCb

ATLAS Electromagnetic Calorimeters

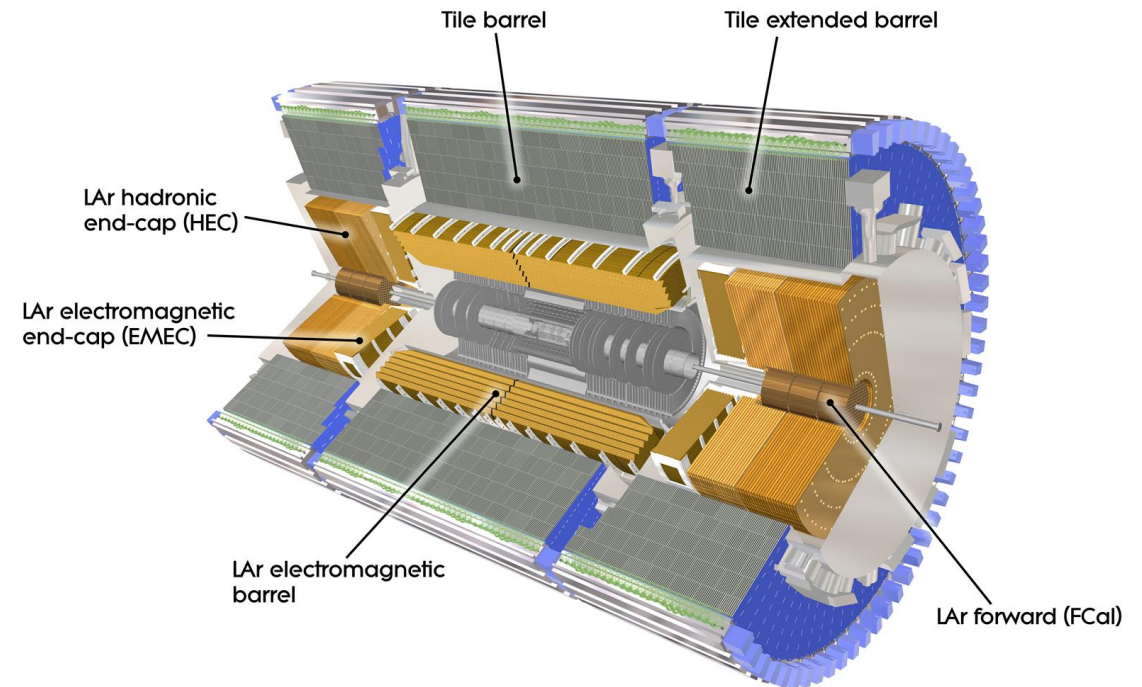
The design for the LAr calorimeter of ATLAS was largely motivated by requirements on searches for the Higgs boson, in which the final state contains photons, electrons, jets and missing energy

Required energy resolution:

- **Sampling term of $< 10\%$** for the electromagnetic calorimeter
- **Constant term (dominates at high energy) $< 0.7\%$** for the electromagnetic calorimeter

The ATLAS calorimeter is a LAr sampling calorimeter consisting of four sub-systems:

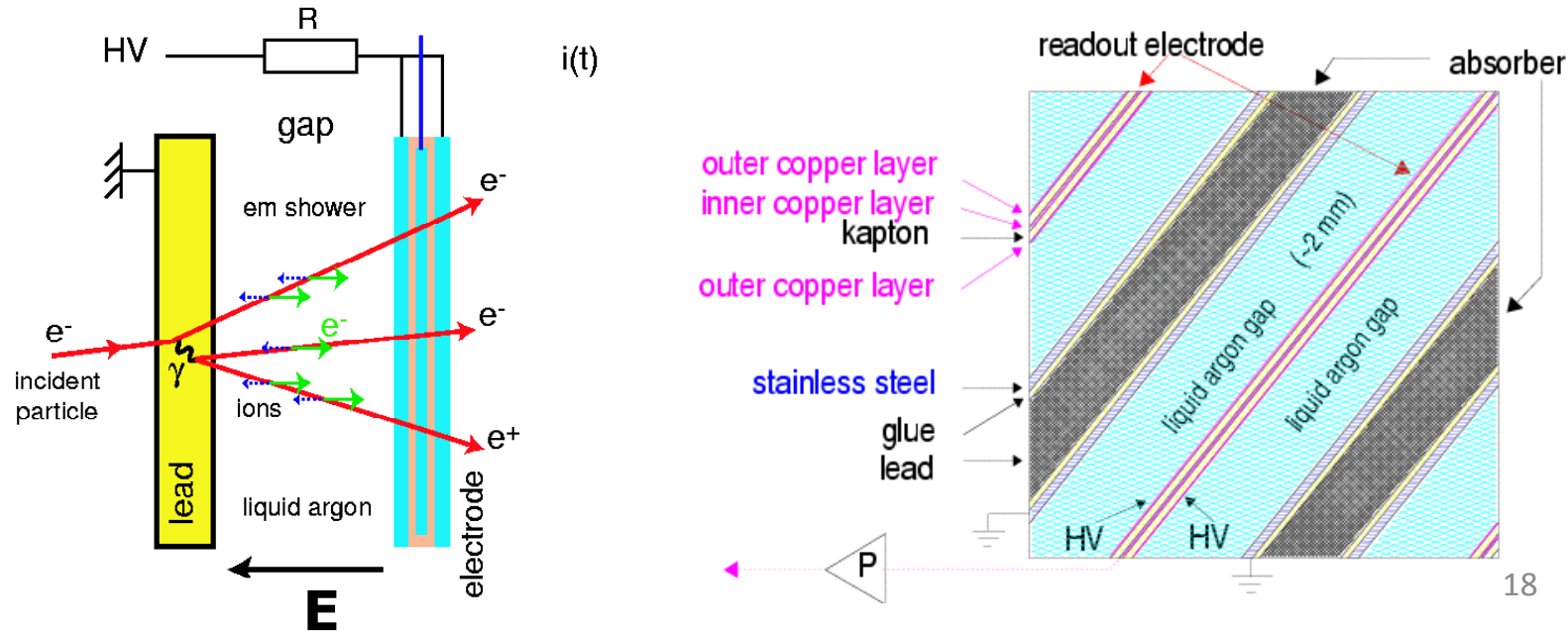
- Electromagnetic barrel (**EMB**): $|\eta| < 1.475$
- Electromagnetic endcap (**EMEC**): $1.375 < |\eta| < 3.2$
- Hadronic endcap (**HEC**): $1.5 < |\eta| < 3.2$
- Forward calorimeter (**FCal**): $3.1 < |\eta| < 4.9$



ATLAS LAr Calorimeter

Sampling Calorimeter: Liquid Argon (active material) and Lead (Absorber)

Operated in a Cryostat < 88K to keep Argon in liquid phase



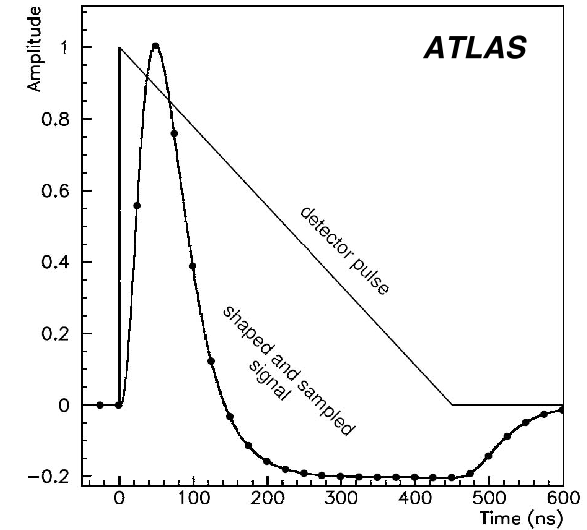
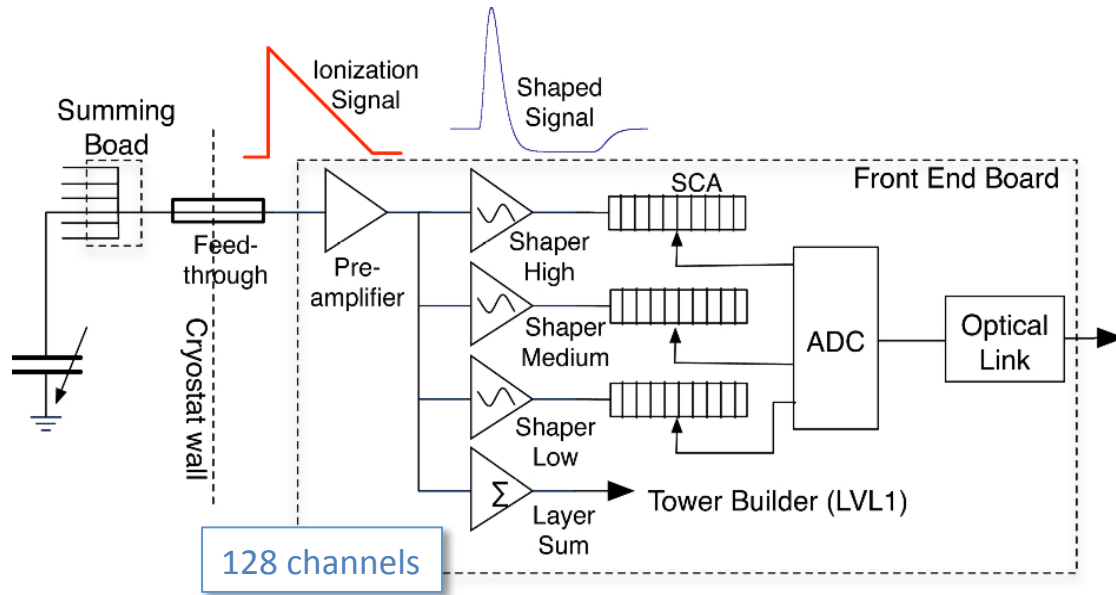
$$I(t) = \frac{dQ(t)}{dt} \propto Q_0 \left(1 - \frac{v_d}{d} t \right)$$

$$t_{\text{drift}} \sim 450\text{ns}$$

Principle of operation

- Interaction mainly in lead absorber
- Charged particles ionize Ar atoms, ionization charge drift in LAr gap where an electric field is applied
- Signal is induced on the readout electrodes by the moving electrons
- Induced signals have a characteristic triangular shape current peak, proportional to energy lost by particle

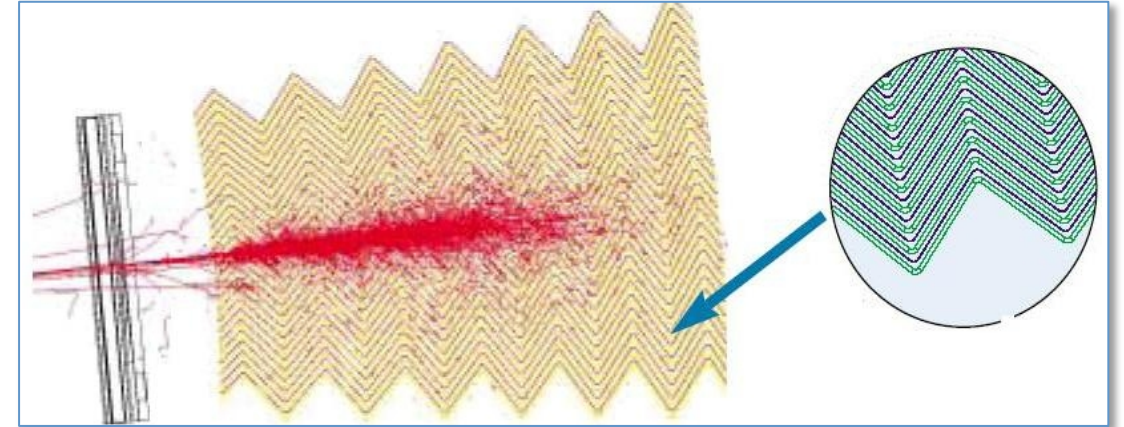
ATLAS LAr Calorimeter – Front-end and Readout electronics



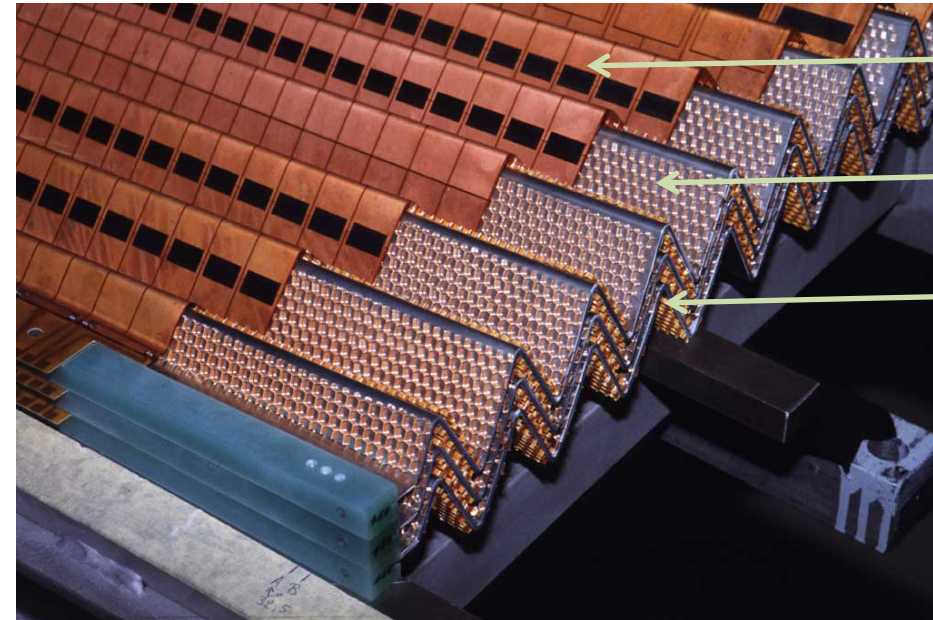
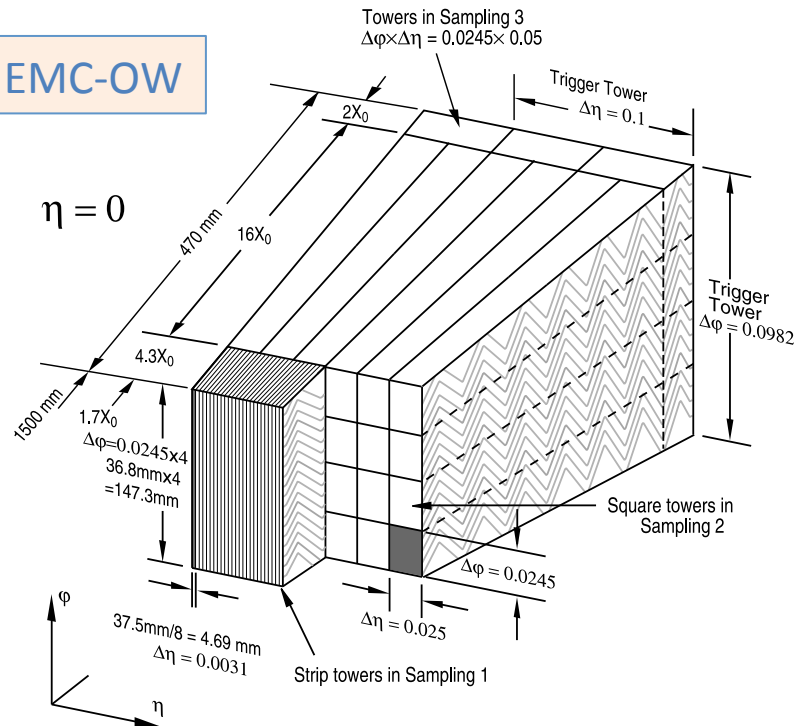
- 3 gains to cover a large dynamic range: low gain / medium gain / high gain $\sim 1 / 9 / 80$
- Shaper: bipolar CR (RC)²
- analogue pipeline (switched capacitor array) to cover L1 trigger latency
- ADC: 12-bit, 40 MHz
- For each L1-triggered event: optimal gain signal is selected and 4-5 samples are digitized and transmitted off-detector via an optical link

ATLAS LAr Calorimeter

- Length: at least $22 X_0$ (47cm)
- 3 longitudinal layers (+pre-sampler)
- $4 X_0$ rejection of π^0 in two γ
- $16 X_0$ for shower core (largest fraction of energy)
- $2 X_0$ evaluation of late showers (shower tail)



EMB, EMC-OW



Copper/Polyimide electrode

Honeycomb spacer

Stainless-steel clad Pb absorber plates

ATLAS LAr Calorimeter

LAr as an active material

- It is **dense**: $1.4\text{g}/\text{cm}^3$
- **relatively high electron mobility**: $\sim 5\text{ mm}/\mu\text{s}$ at $1\text{kV}/\text{mm}$
- **A good ionization yield**: ionization potential of 23.6 eV
- It is easy to obtain and purify: **relatively low cost** compared to e.g. liquid krypton or liquid xenon)
- It is **radiation hard**
- **“slow”** charge collection: $v_{\text{drift}} = 450\text{ns} \gg 25\text{ns}$ (LHC BC frequency)
- **Cryogenics**: difficult operation, additional dead material

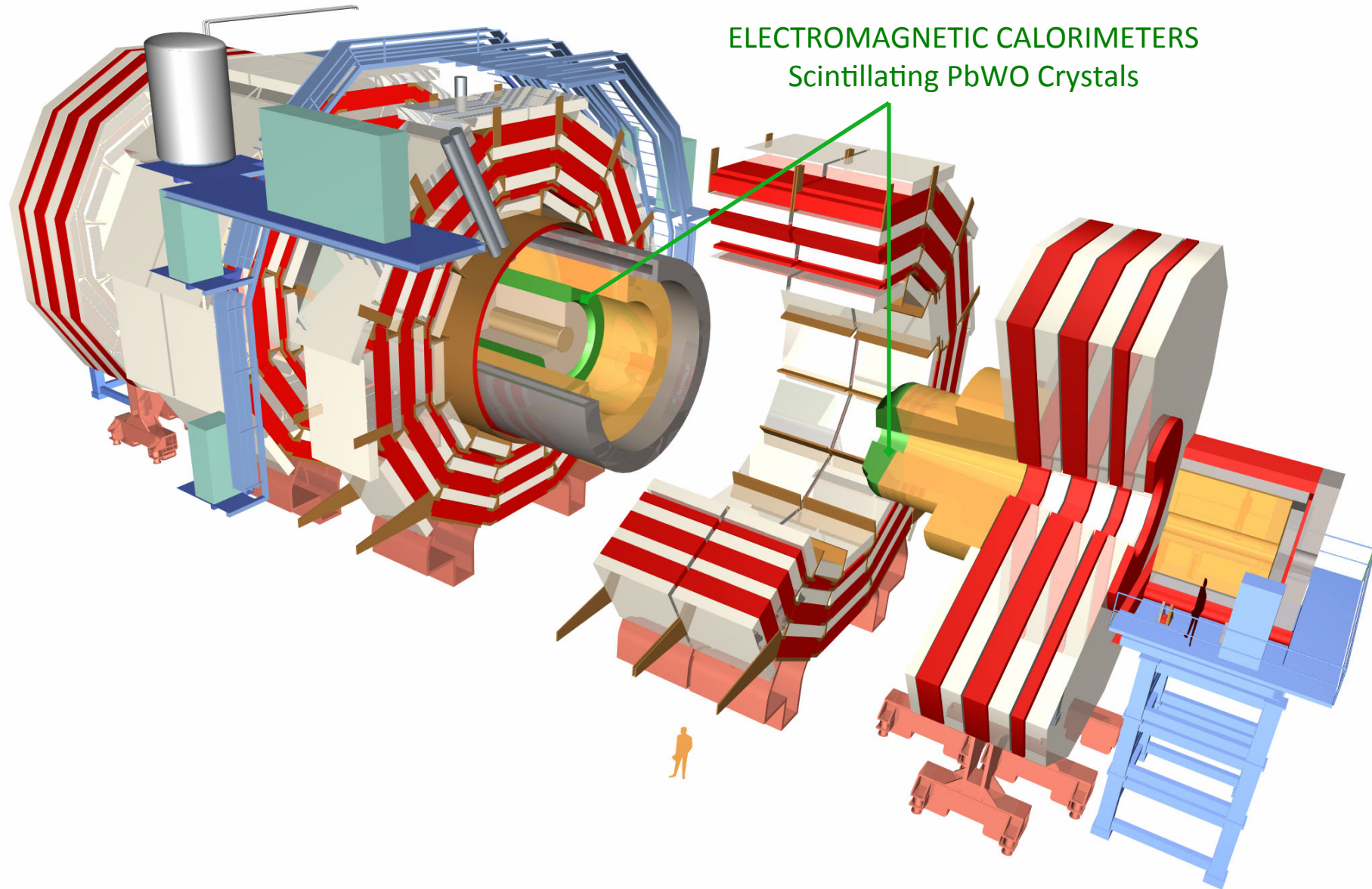
Pb as an absorber

- **short radiation length** (0.56 cm) \rightarrow compact calorimeter
- It is easy to machine, **cheap and radiation hard**
- **Relatively non-toxic**

Very good electromagnetic calorimetry
identification and energy measurement
over a large dynamic range

$50\text{MeV} \rightarrow 1\text{Tev} : 16\text{ bit}$

CMS Electromagnetic Calorimeters



CMS Electromagnetic Calorimeter

Primary Detection Material

Lead-tungstate crystals (PbWO_4)

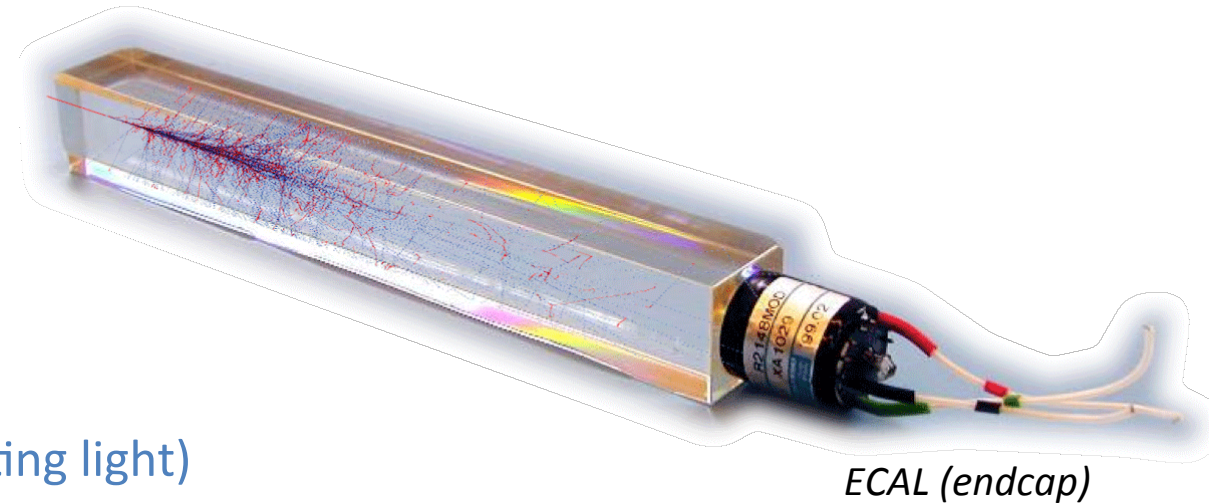
Characteristics: dense, fast, relatively radiation hard

- Radiation Length $X_0 = 8.9$ mm
- Moliere radius $R_M = 22$ mm
- Emission spectrum 420-550nm (blue-green scintillating light)
- Fast: 80% of light emitted within 25ns (comparable to LHC bunch-crossing time)
- Radiation-hard – up to 10Mrad

★ But light yield relatively low and strongly temperature dependent: $-2.2\% / ^\circ\text{C}$

Photo-detectors

- Mounted onto backside of each crystal
- Barrel: 2 x silicon avalanche photodiodes (APDs)
- Endcap: vacuum phototriodes (VPTs)
- QE (@420nm): 80% (APD), 15% (VPT)
- Temperature sensitivity: $-2.2\% / ^\circ\text{C}$



Endcap has also preshower detector

- Sits inside endcap crystal array
- Sampling calorimeter
- Lead “radiator” + silicon strip sensors (2 layers)

➔ need to stabilize crystal volume temperature to $0.1 ^\circ\text{C}$

CMS Electromagnetic Calorimeter



CERN Labo 27 – EP/CMA
09/07/2002 – 3

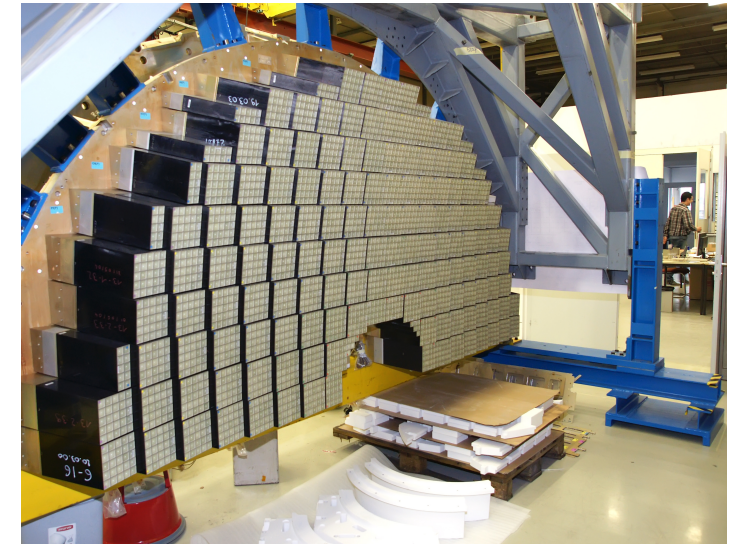


Barrel Section

- Range: $0 \leq |\eta| \leq 1.497$
- Inner radius: 1.29 m
- 61,200 crystals = 360 (around ϕ) x 170 (along z)
- Cross section $22 \times 22\text{mm} = 1 \times 1 R_M$
- Length: $230\text{mm} = 25.8 X_0$
- Most energy (94%) from a single particle contained in 3×3 crystals

Endcap Section

- 2 x endcaps, containing 7324 crystals each
- Cross-section: $28.6 \times 28.6\text{mm} = 1.3 \times 1.3 R_M$
- Length: $220\text{mm} = 24.7 X_0$
- Most of energy also contained in 3×3 crystals



Electromagnetic Calorimeter – Test beam performance

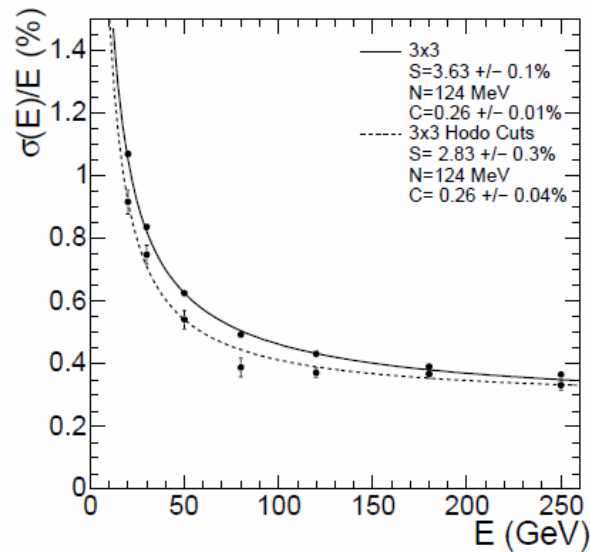
Energy resolution

$$\frac{\sigma_E}{E} = \frac{a}{\sqrt{E}} \oplus \frac{b}{E} \oplus c$$

CMS – homogeneous PbWO_4

a = stochastic term = $3.63 \pm 0.1\%$

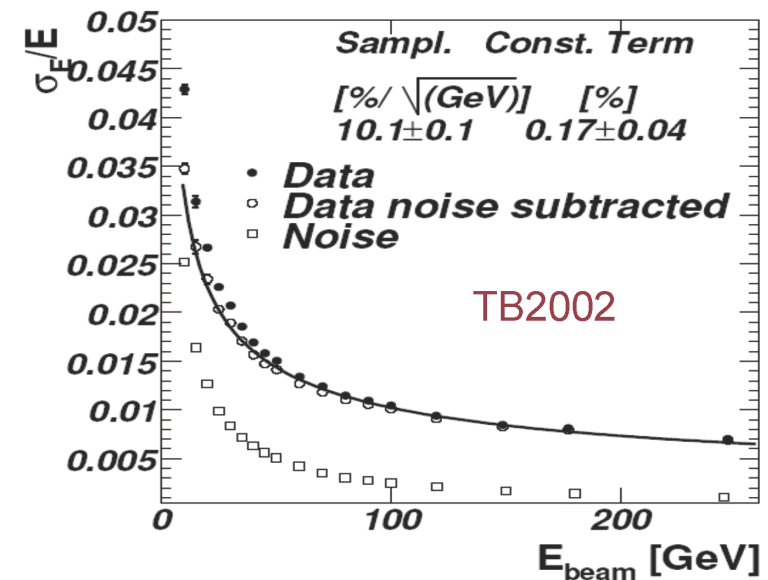
c = constant term = 0.26 ± 0.01



ATLAS – sampling Pb-LAr

a = stochastic term = $10.1 \pm 0.1\%$

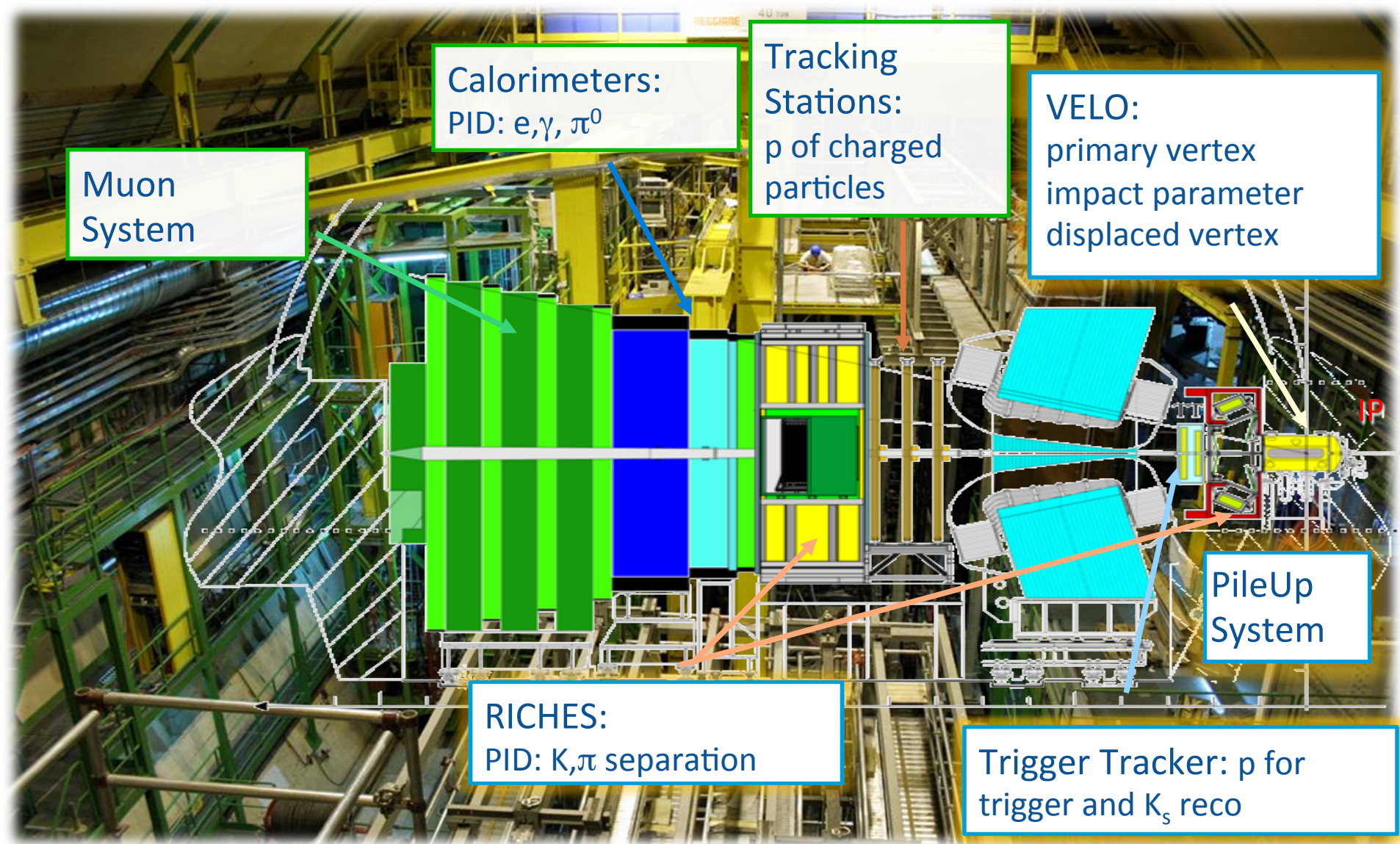
c = constant term = 0.17 ± 0.04



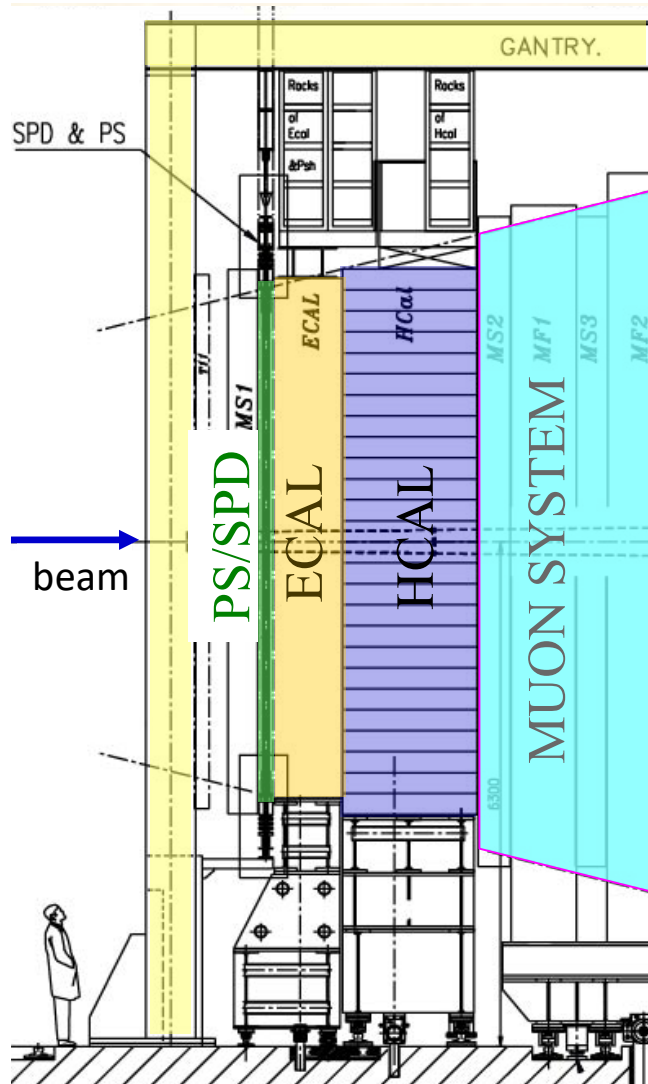
Electron test-beam

Global Constant Term 0.6-0.7%

LHCb Calorimeters



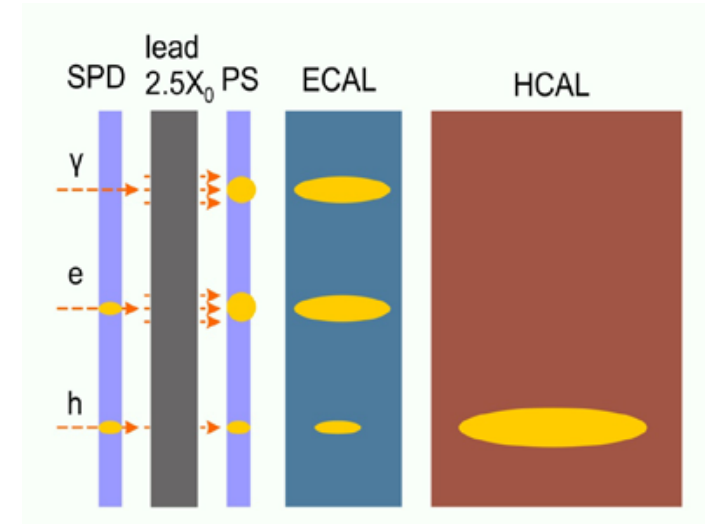
The LHCb Calorimetry System



- Solid angle coverage: 300 x 250 mrad
- Distance from IP: ~12.5m

Four Subdetectors

- SPD: Scintillating Pad Detector
- PS: scintillating pads (preshower)
- ECAL: “shashlik”- type
- HCAL: scintillating tile iron plate



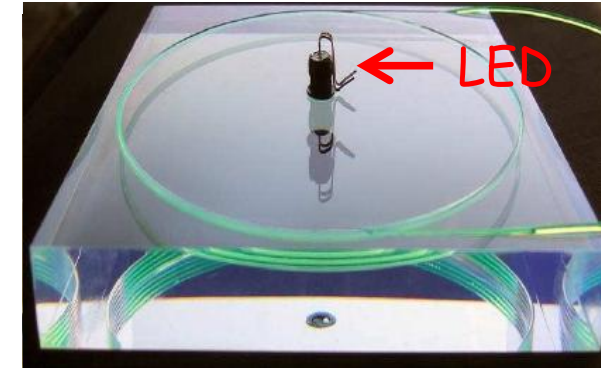
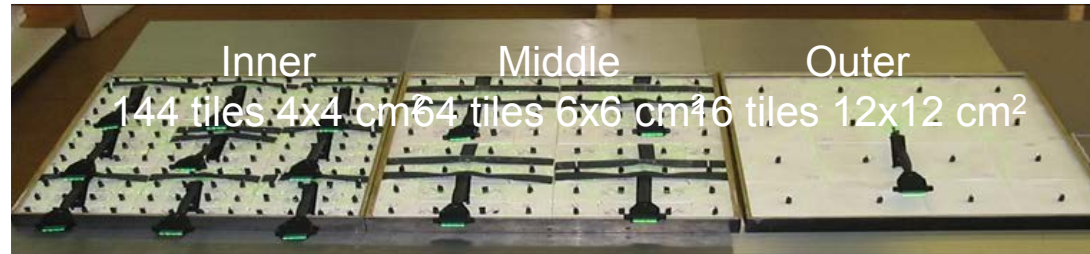
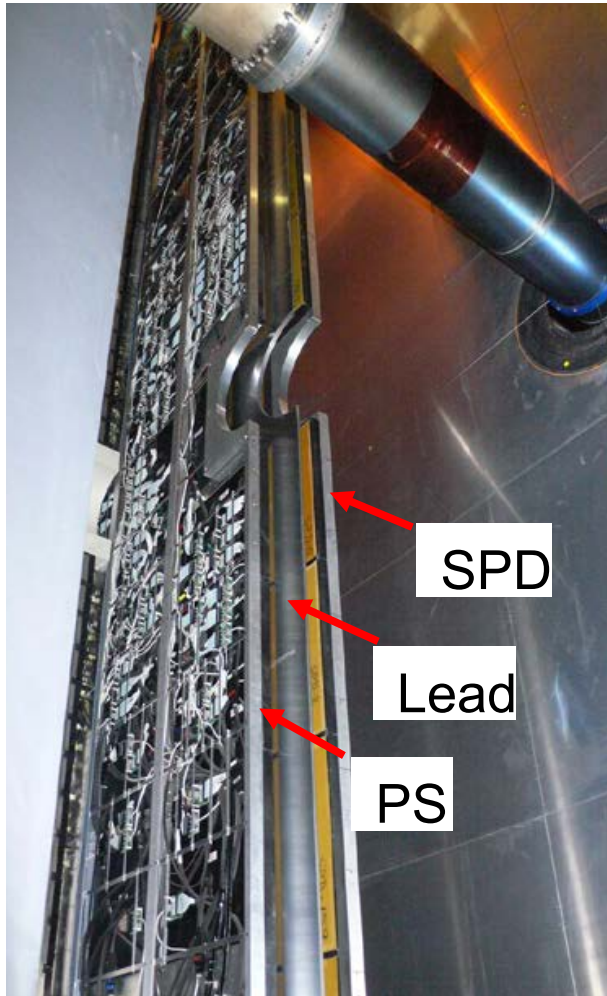
Based on **scintillation/WLS** technique, light readout with **PMT**

Provides

- L0 trigger on high p_T e^\pm , π^0 , γ , hadron
- energy measurement of e^\pm and γ
- Particle identification: e^\pm/γ /hadron

LHCB Calorimeters - PS and SPD

Preshower detector: two planes of scintillator tiles (15mm thick) with one lead plane (15mm thick) between them. Size and segmentation match ECAL

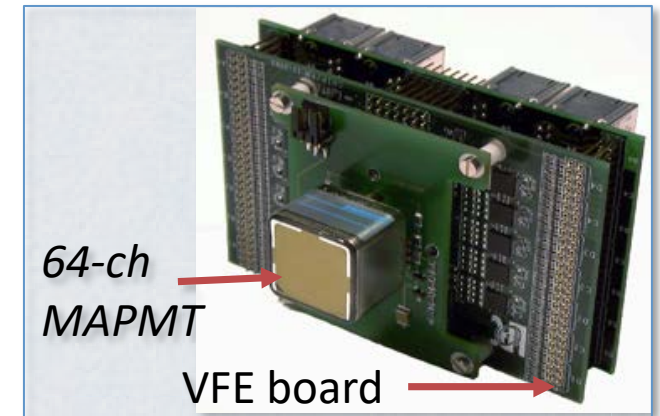


The light is captured and re-emitted by **WLS fibers** (3.5 loops) glued in a deep groove machined at the surface of the tile. The light is transported via clear fibers to a **64-channel multi-anode PMT (HAMMAMATSU)**

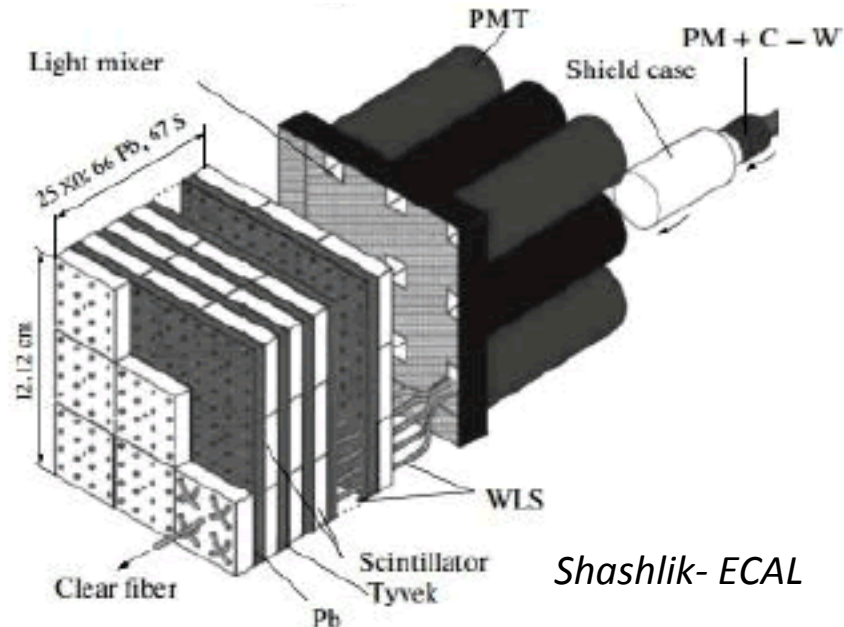
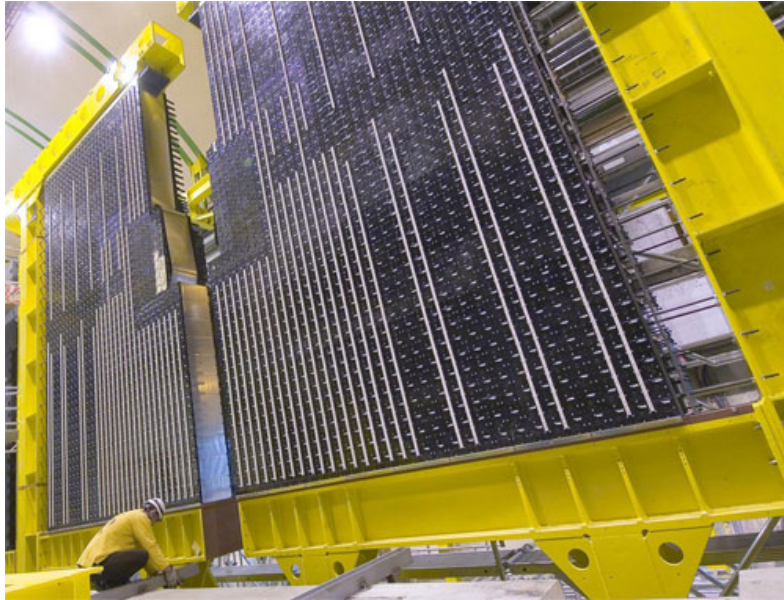
Tiles are equipped with LED monitoring system

Light yield measured for all 12032 cells with cosmics during the production:

$$\sim 25 \pm 12 \text{ ph.el. /MIP}$$



LHCb Calorimeters - ECAL



Shashlik- ECAL



Shashlik technology

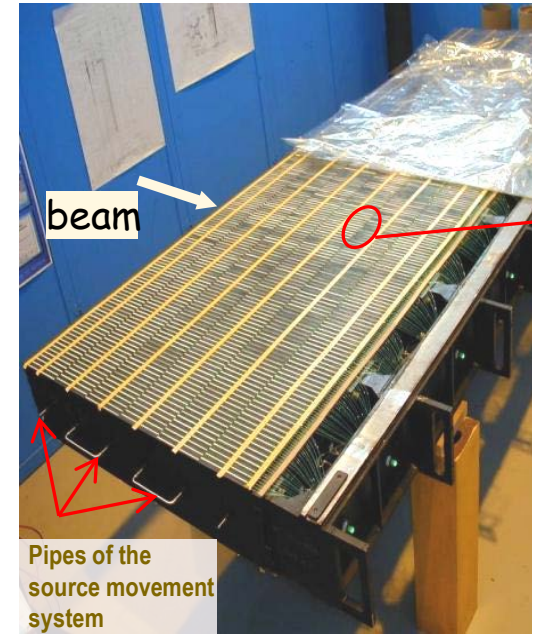
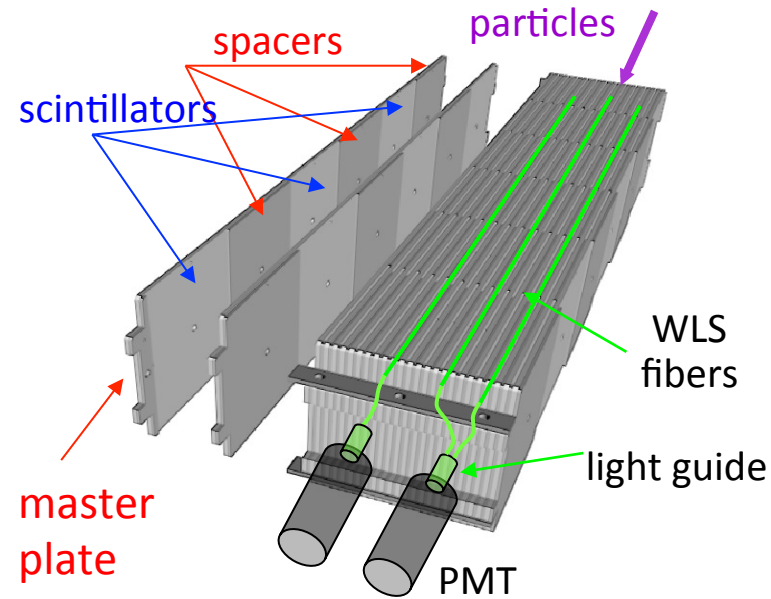
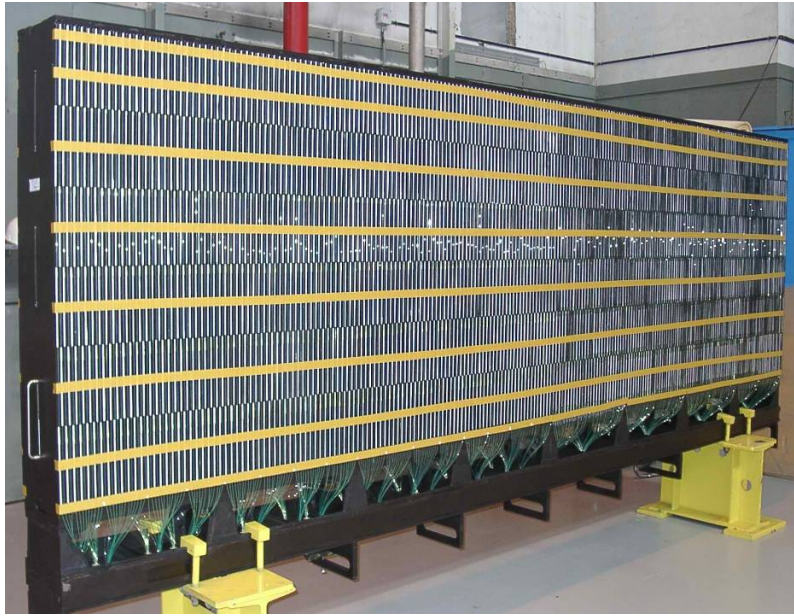
- 4mm thick scintillator tiles and 2mm thick lead plates, $25 X_0$ ($1.1 \lambda_1$); Moliere radius $\sim 36\text{mm}$
- Modules $121.2 \times 121.2 \text{ mm}^2$, 66 Pb + 67 scintillator tiles;
- Segmentation: 3 zones (inner, middle and outer with 9, 4, 1 cells/module respectively)
- Total of 3312 modules, 6016 cells, ~ 100 tons
- Light readout: PMT (HAMAMATSU)

Average performance figures from beam test
(slight difference between zones)

Ligh yield: 3000 ph.el. / GeV

Energy resolution $\frac{\sigma_E}{E} = \frac{(8 \div 10)\%}{\sqrt{E(\text{GeV})}} \oplus 0.9\%$

LHCb Calorimeters - HCAL



Tilecal technology (originally developed for ATLAS)

- The volume ratio Scint:Fe $\sim 3:16$
- Instrumented depth: 1,2m, 6 tiles rows, $\sim 5.6\lambda_i$
- Outer cells: 26x26 cm², Inner: 13x13 cm² (half tiles)
- Total of 1488 cells, 2x26 modules, 500 tons
- Scintillator, fibers, PMTs, LED system: similar to ECAL

Average performance figures from beam test

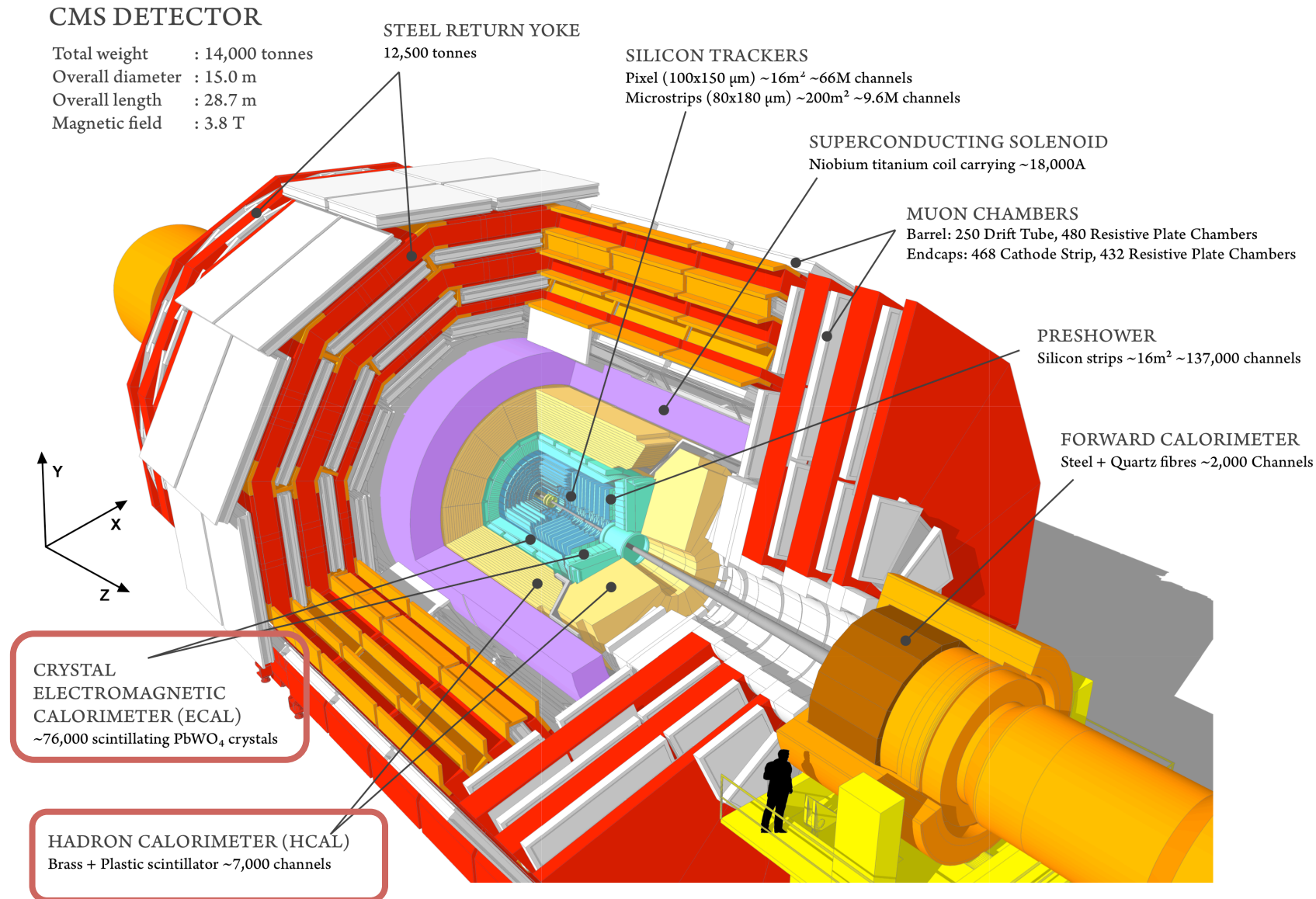
Ligh yield: 105 ± 10 ph.el. / GeV

Energy resolution
$$\frac{\sigma_E}{E} = \frac{(69 \pm 5)\%}{\sqrt{E}} \oplus (9 \pm 2)\%$$

Silicon Detectors in Calorimetry

CMS High Granularity ECAL

HGC – The CMS High Granularity Calorimeter for HL-LHC



HGC – The CMS High Granularity Calorimeter for HL-LHC

HL-LHC presents increased challenges for triggering, tracking and calorimetry, in particular for low to medium p_T objects in the End-Caps

- Higher radiation load
- Higher particle density
- Higher multiplicity

The End-Cap regions will be particularly stressed

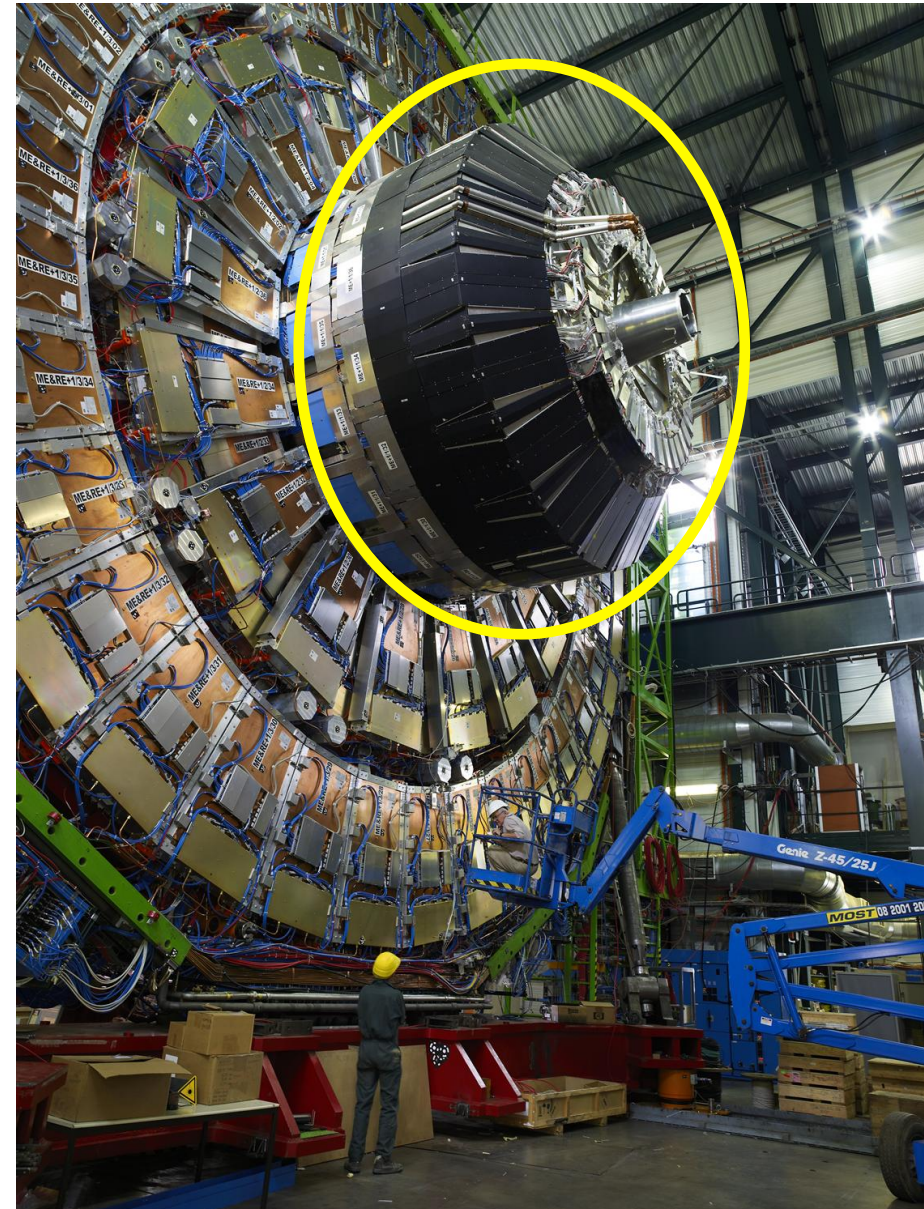
Improve calorimeter coverage in the forward region



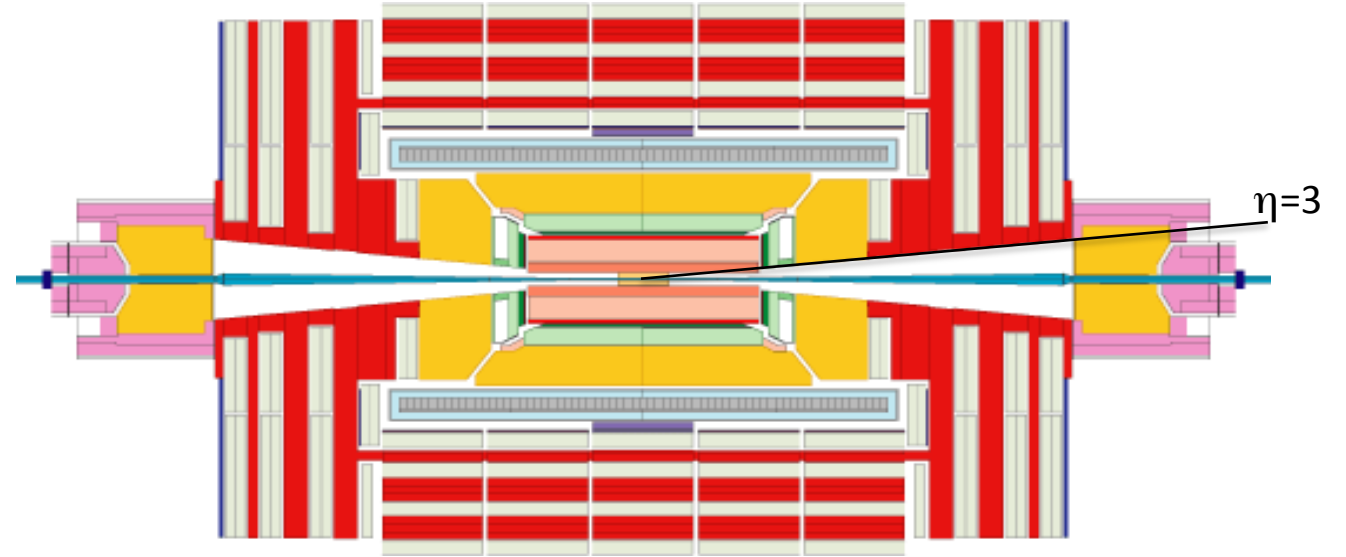
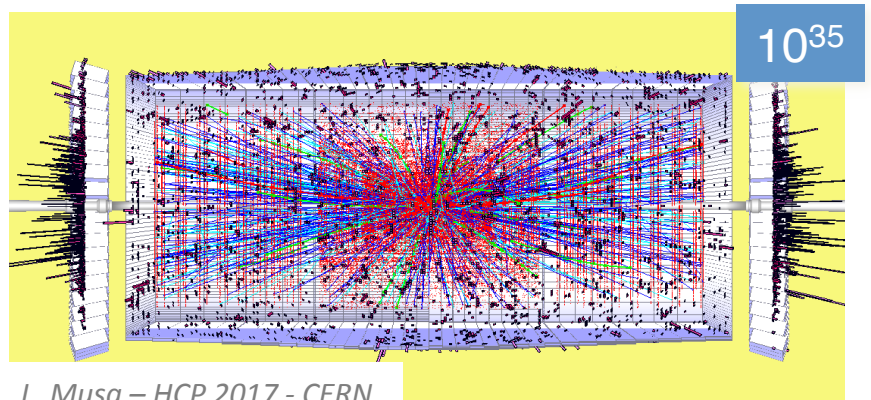
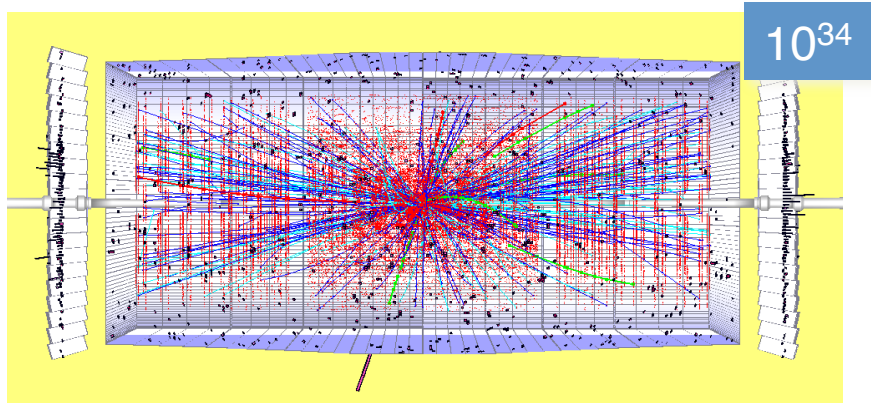
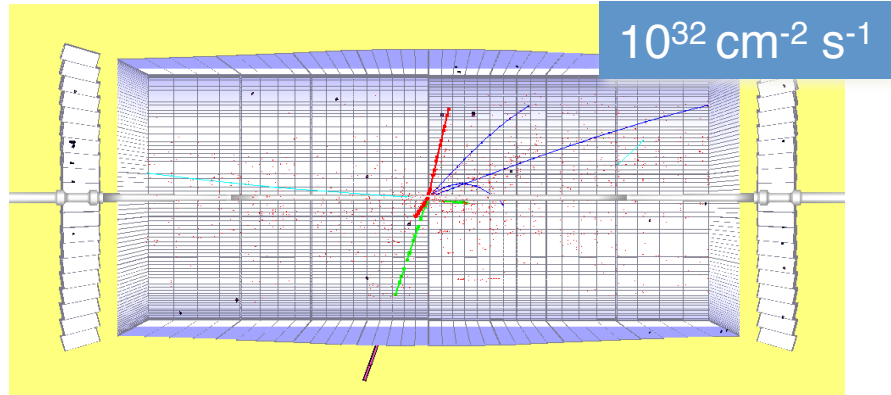
CMS End-Cap Calorimeters need to be replaced

An entirely new highly segmented sampling calorimeter based on Si PADs is being developed

precision timing in association with the calorimeters as a means to mitigate PU for neutral particles is also being considered



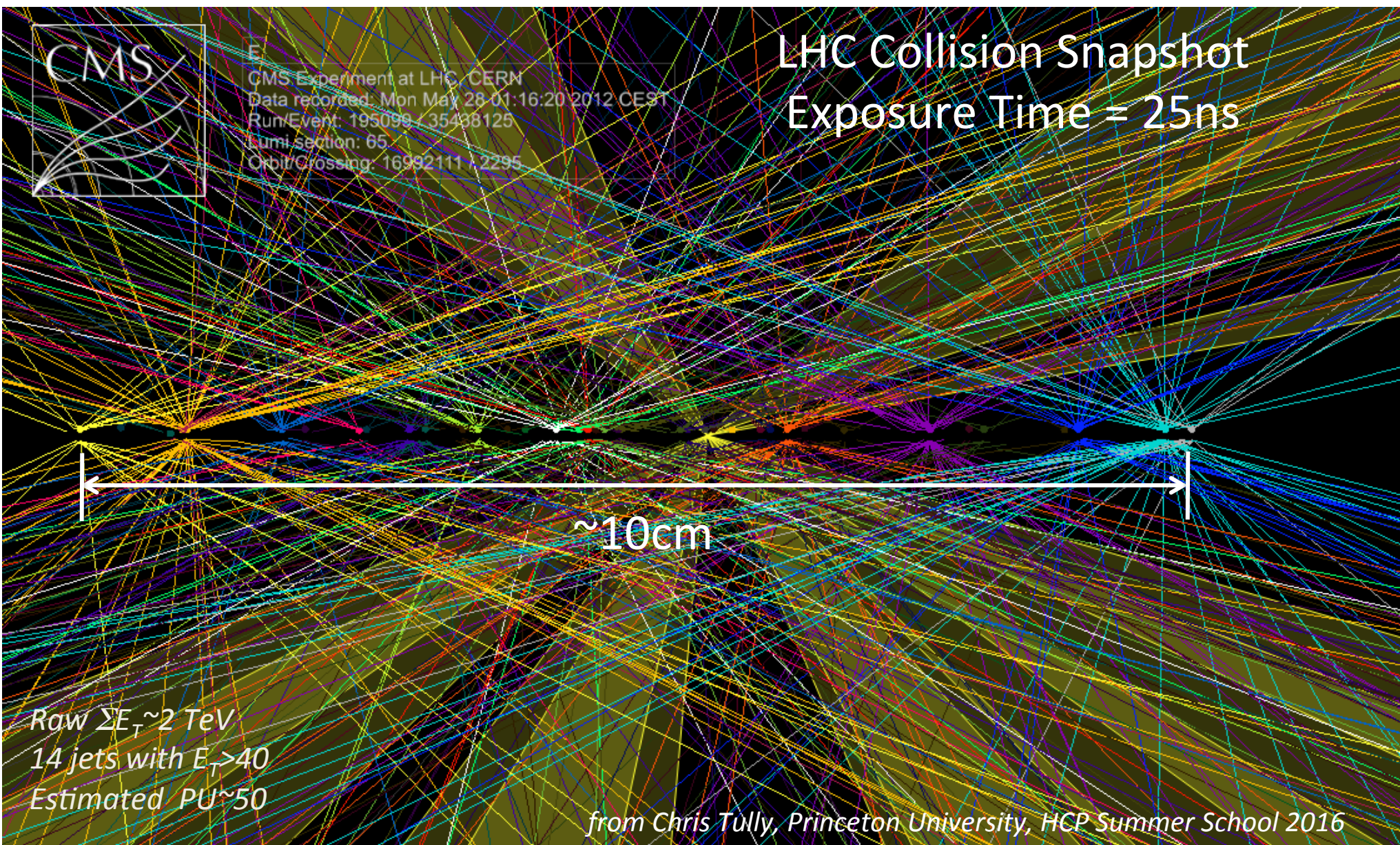
HGC – The CMS High Granularity Calorimeter for HL-LHC



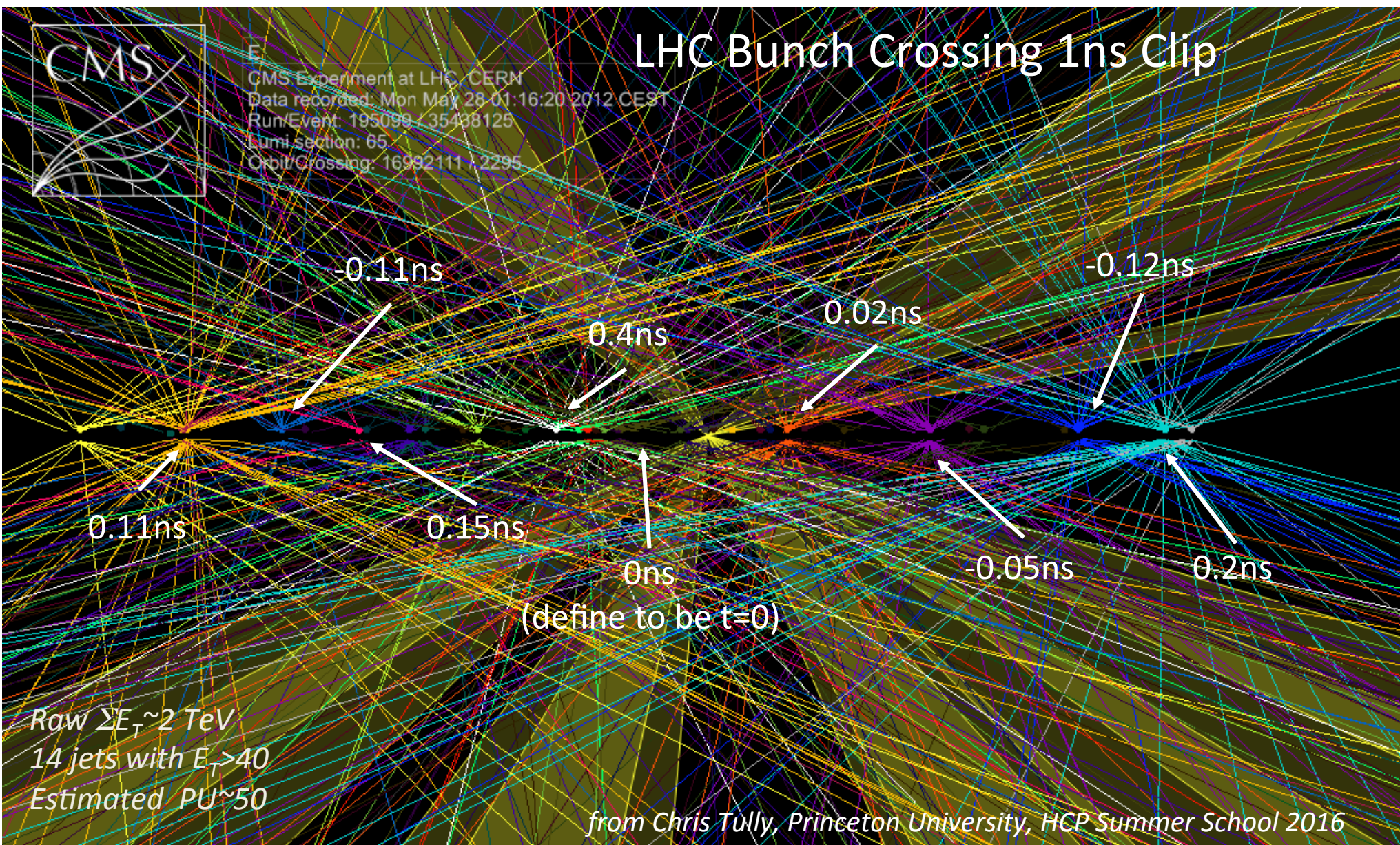
Measurement of Vector Boson Fusion (VBF) jets
⇒ very important at HL-LHC

- Quarks do not interact through color exchange i.e. the jets are peaked in forward direction at $\eta=3$.
- Signature: high jet activity in forward region, little hadronic activity in the barrel
- $\eta = 3$ is exactly in the transition region of the End-Cap calorimeters !

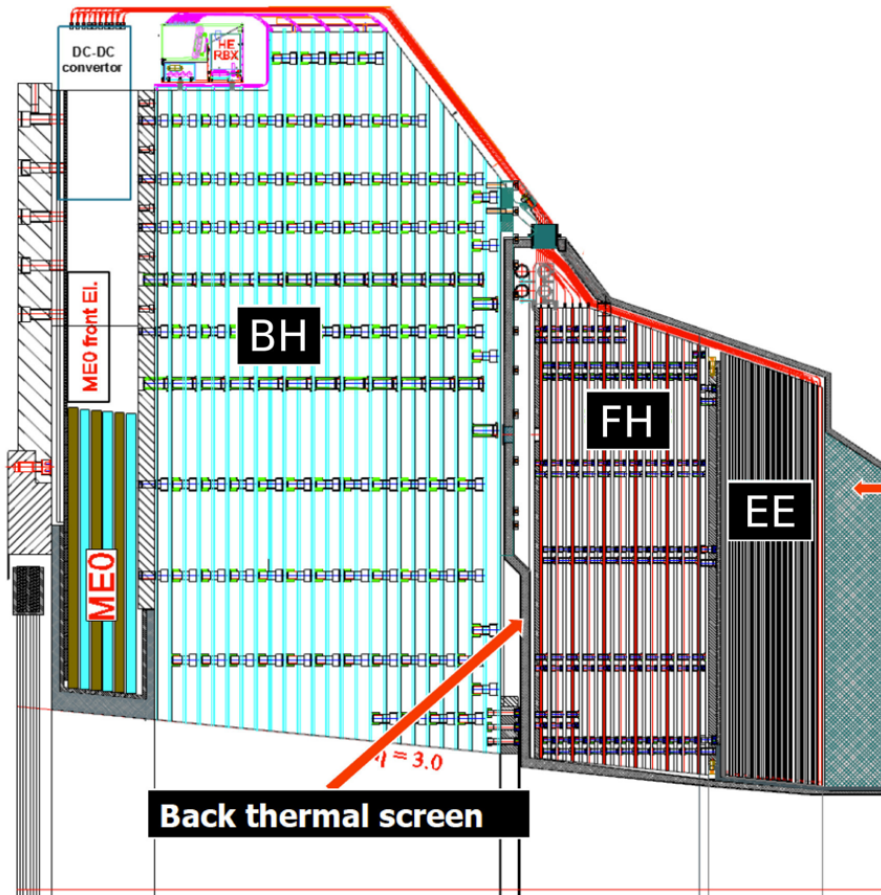
How to resolve event pile-up - Vertex Spacing



How to resolve event pile-up - Vertex Spacing



HGC – The CMS High Granularity Calorimeter for HL-LHC



Key parameters

- $\approx 600 \text{ m}^2$ of silicon
- 6M ch, 0.5 or 1 cm^2 cell-size
- 21,660 modules (8" or 2x6" sensors)
- 92,000 front-end ASICS
- Power at end of life 115 kW

Construction

- Hexagonal Si-sensors built into modules
- Modules with a W/Cu backing plate and PCB readout board
- Modules mounted on copper cooling plates to make wedge-shaped cassettes

System Divided into three separate parts

- EE – Silicon with tungsten absorber – 28 sampling layers – $25 X_0 + \sim 1.3 \lambda$
- FH – Silicon with brass absorber – 12 sampling layers – 3.5λ
- BH – Scintillator with brass absorber – 11 layers – 5.5λ

*EE and FH are maintained at -30°C .
BH is at room temperature*

HGC – A High Granularity Calorimeter for the CMS phase-II upgrade

Hexagonal sensor geometry (based on SiD design): largest tile-able polygon

⇒ maximize use of circular wafer

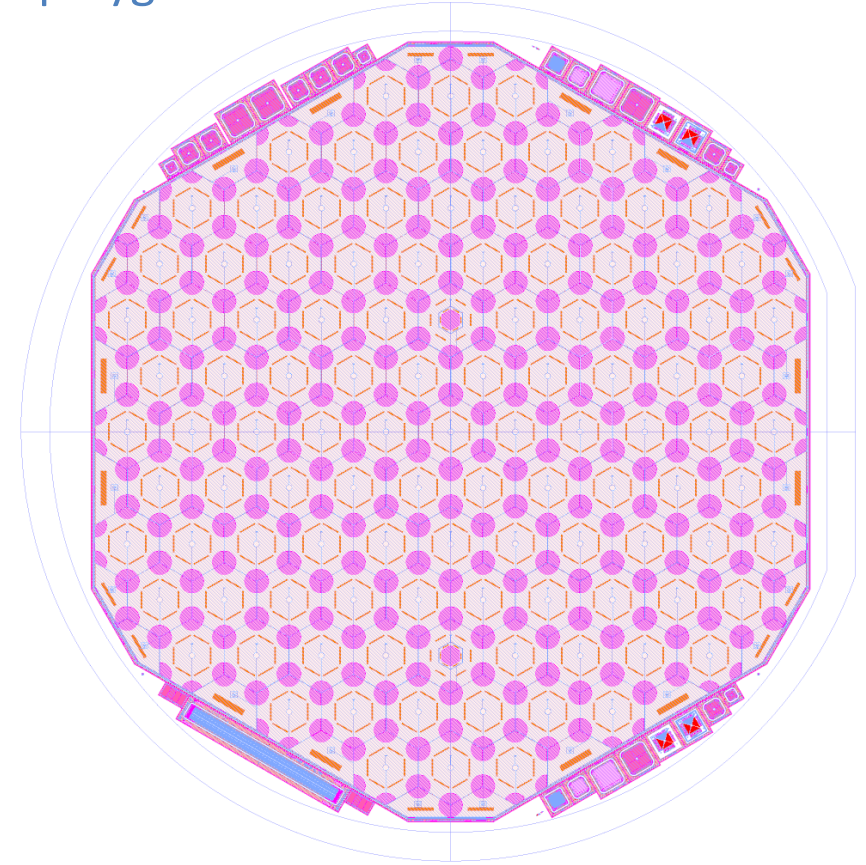
⇒ Minimize ratio of periphery (cracks...) to surface area

Si HGC Sensor

Proposal based on 6" wafer sensor production

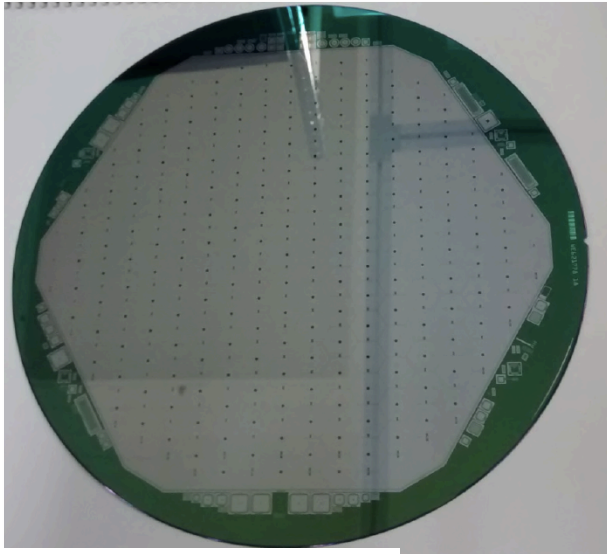
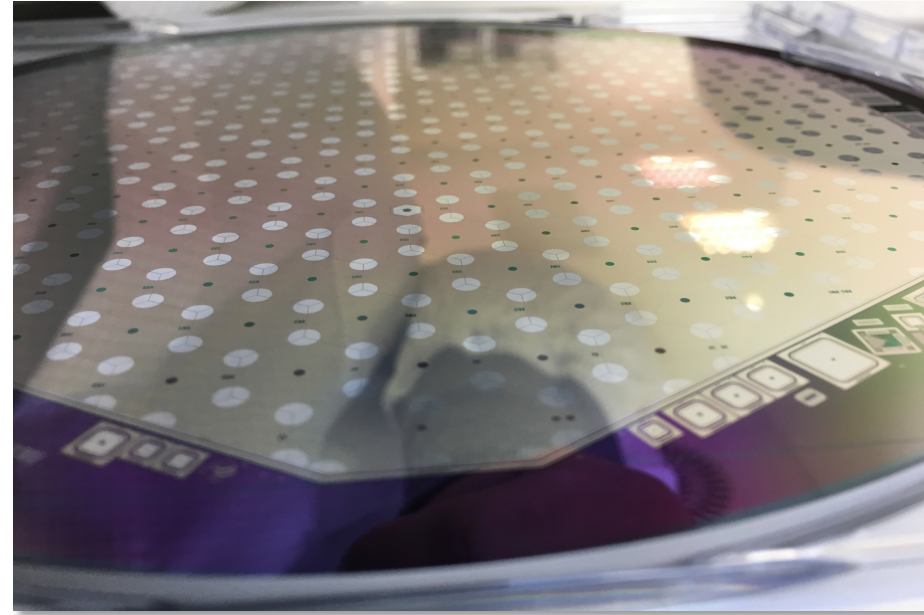
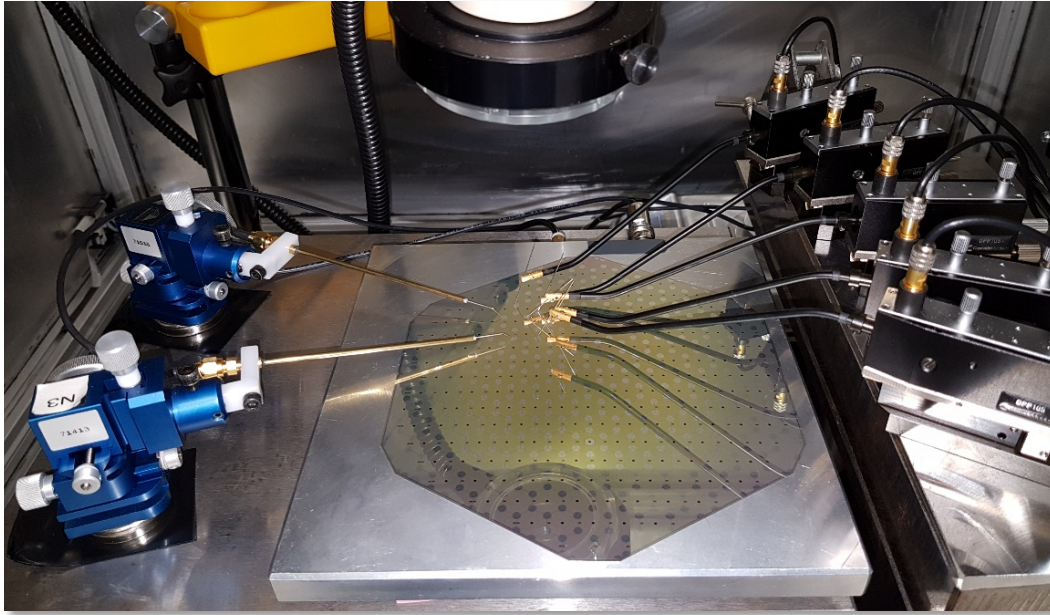
Working with vendors to move to 8" sensor production

- Cell size $\sim 1\text{cm}^2$
- for 300um & 200um thick sensors
 - ⇒ Cell capacitance 40~60pF
- Cell size $\sim 0.5\text{cm}^2$
- for 100um thick sensors
 - ⇒ Cell capacitance $\sim 50\text{pF}$



Truncated tips "mouse-bites" used for module mounting
⇒ Further increase use of wafer surface

HGC – A High Granularity Calorimeter for the CMS phase-II upgrade



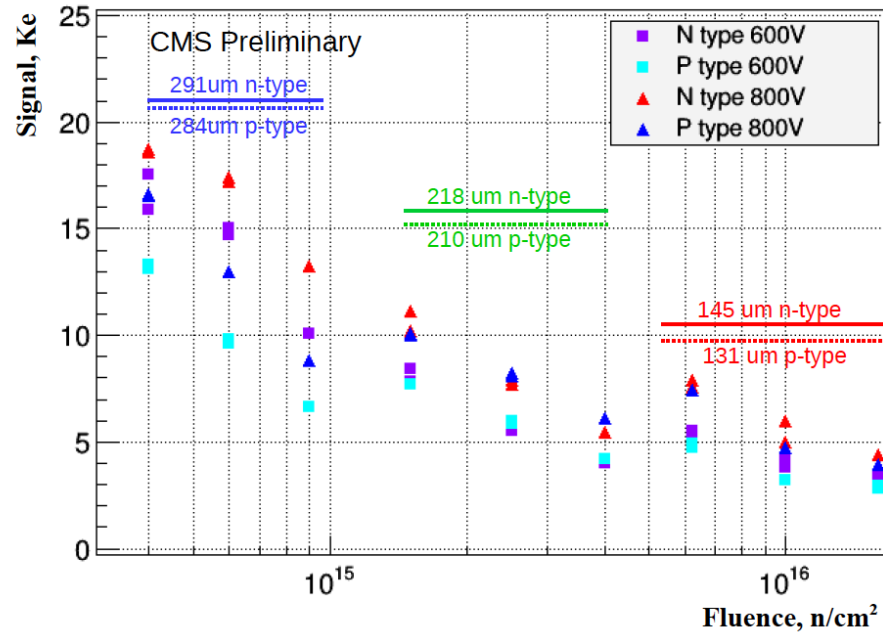
Sensor baseline is n-on-p, but R&D still ongoing

- Chosen by tracker for better noise performance after irradiation
 - Different effect of surface damage for p-on-n / n-on-p
- NMOS input transistors for pre-amp provides best performance
 - Best trans-conductance, noise and power rejection
 - Naturally matched to negative signals

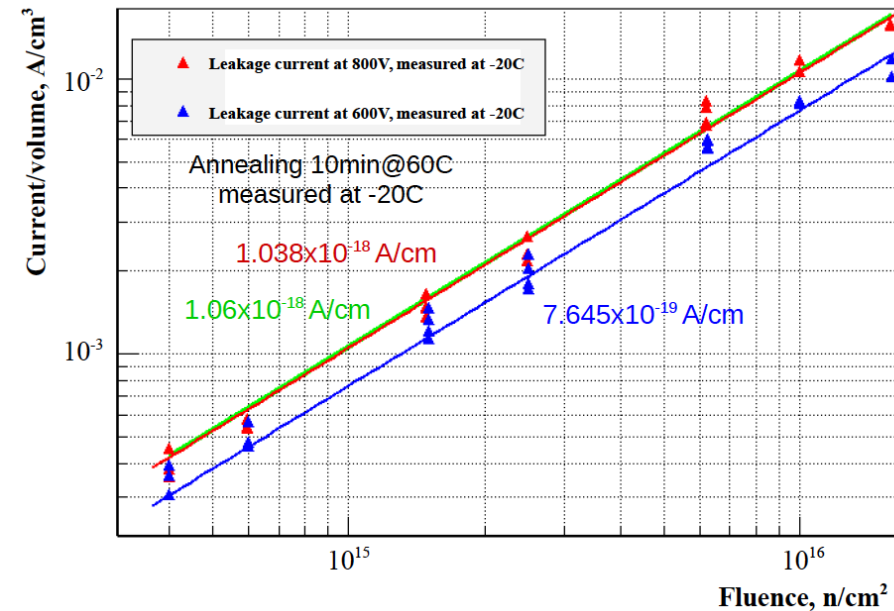
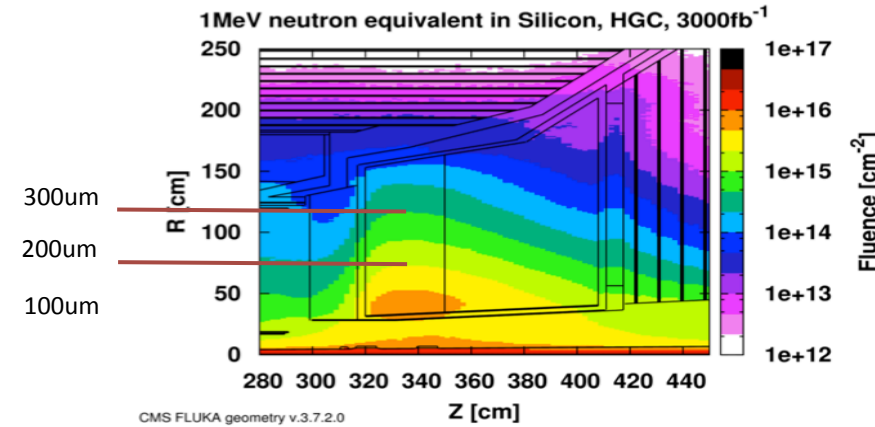
But there could be still some advantage for HGC to use n-on-p sensors: simpler process, better charge collection (especially for 300mm thick sensors)

HGC – A High Granularity Calorimeter for the CMS phase-II upgrade

Basic Silicon Sensor R&D

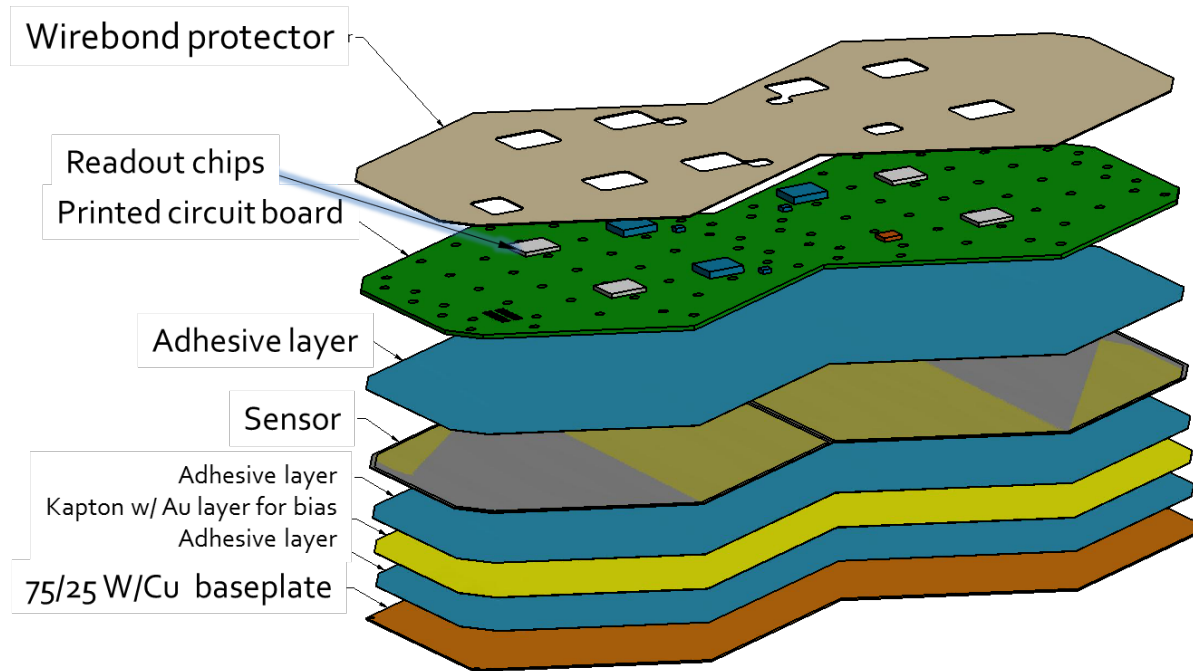


Results documented in
CMS Upgrade Technical Proposal

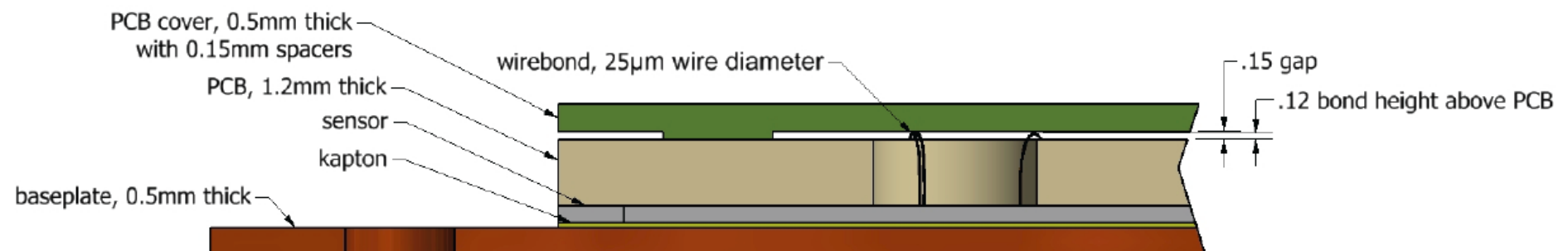
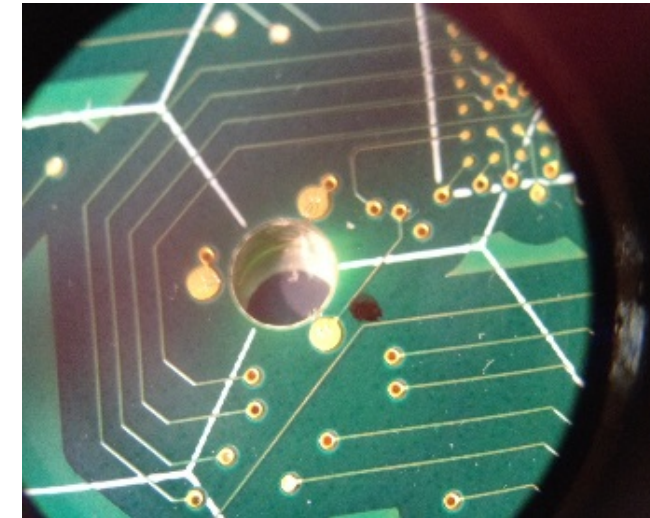


HGC – A High Granularity Calorimeter for the CMS phase-II upgrade

Si HGC Module

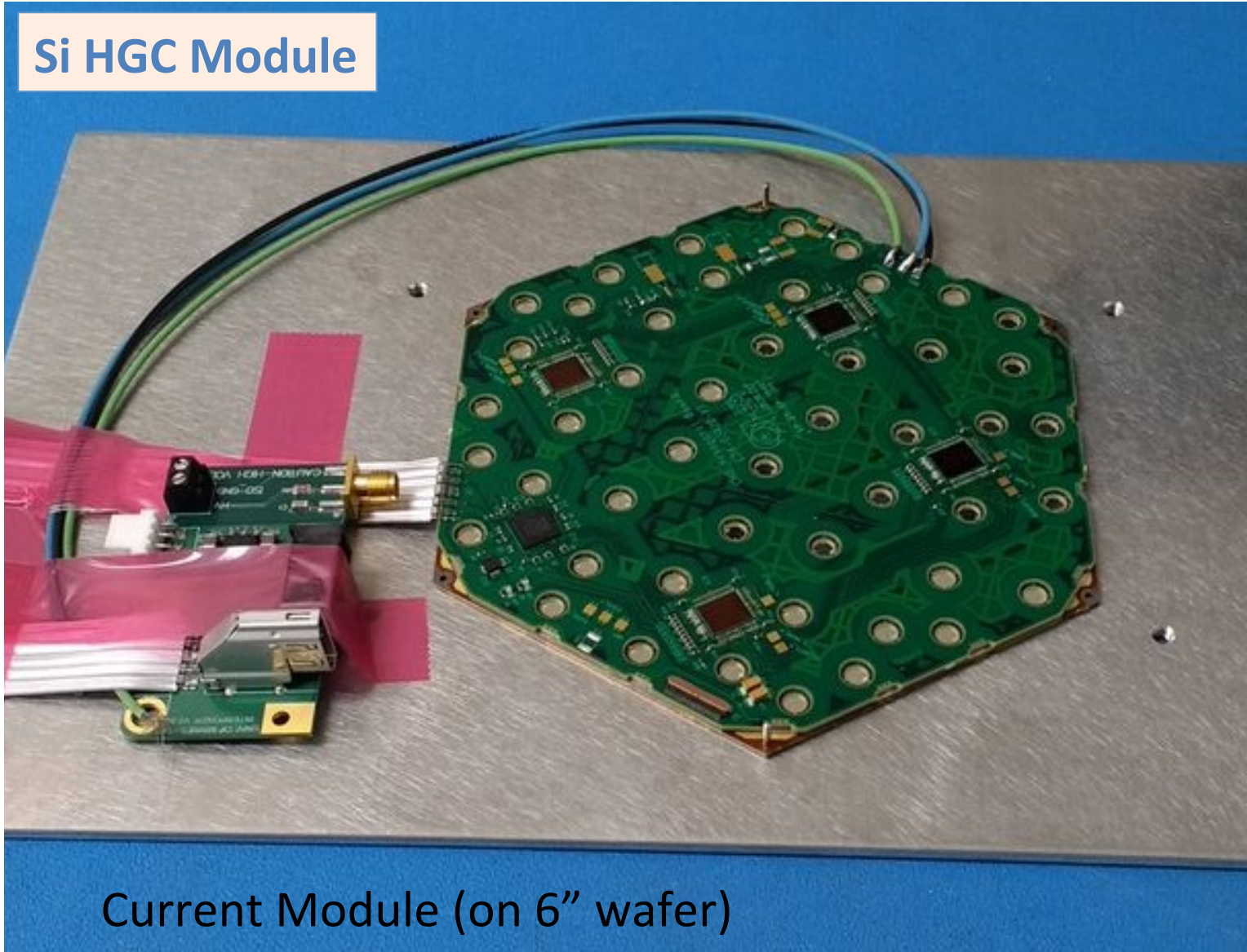


2 sensors per baseplate

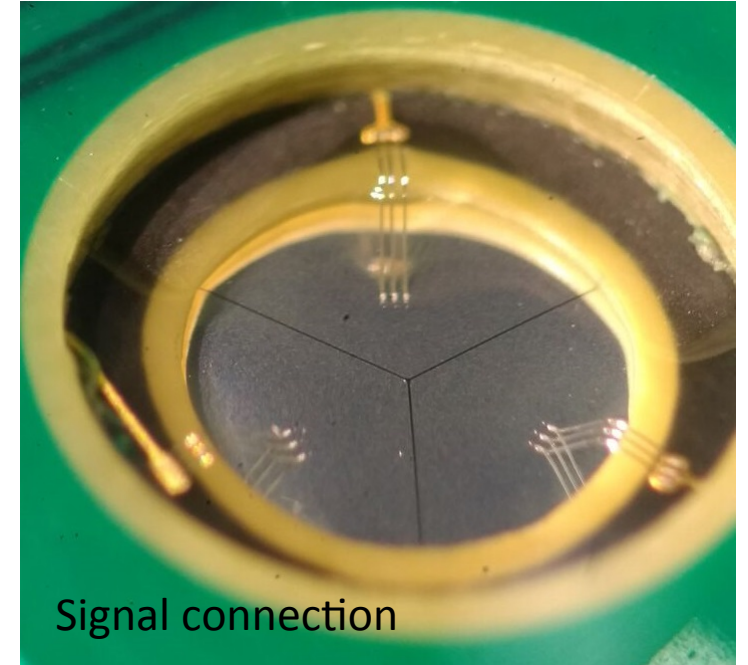


HGC – A High Granularity Calorimeter for the CMS phase-II upgrade

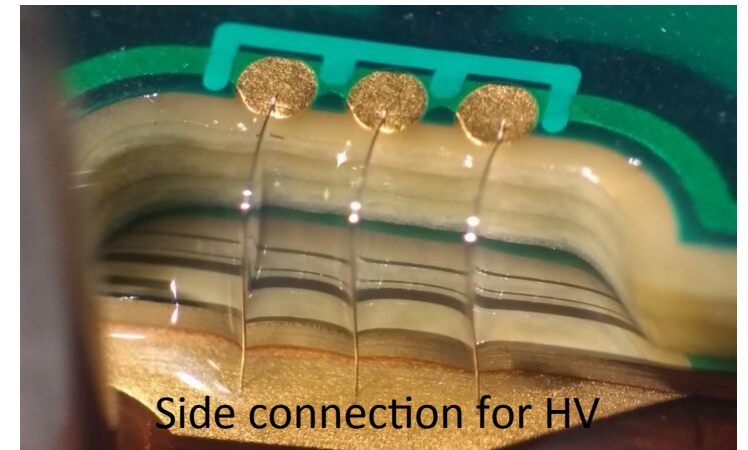
Si HGC Module



Current Module (on 6" wafer)

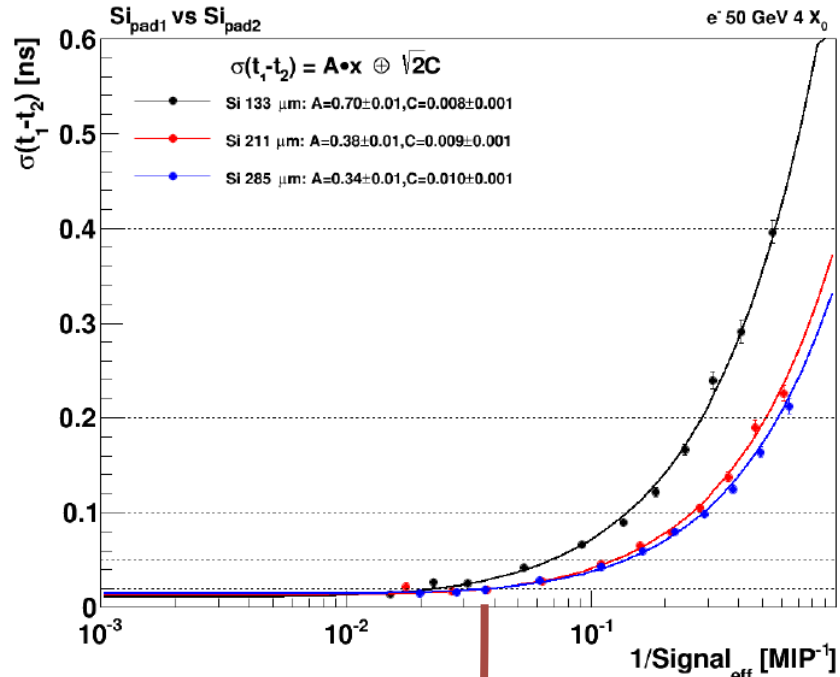


Signal connection

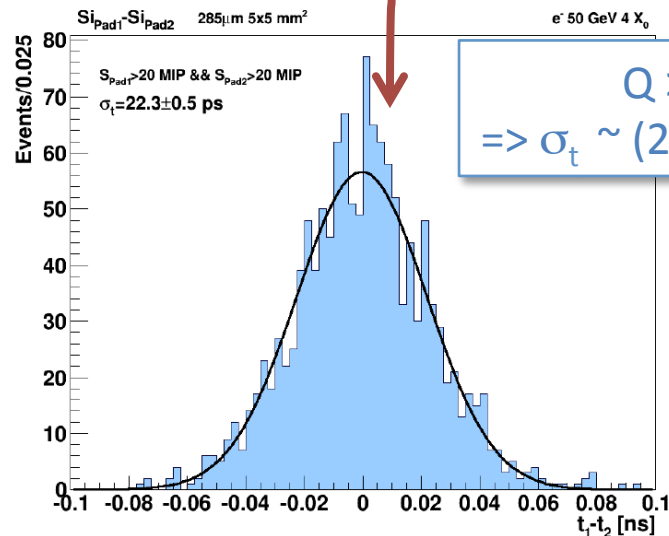
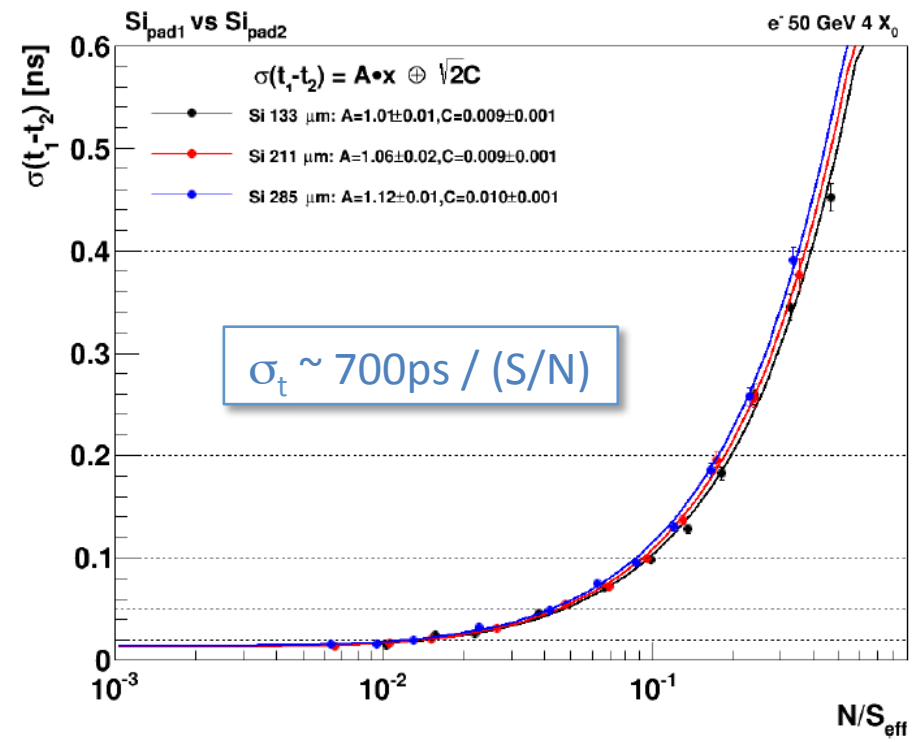


Side connection for HV

HGC – A High Granularity Calorimeter for the CMS phase-II upgrade



HGC Test Beam
Timing Studies



$Q > 20 \text{ MIP}$
 $\Rightarrow \sigma_t \sim (22\text{ps} / \sqrt{2}) \sim 15\text{ps}$

$\sigma_t < 50 - 20 - 10 \text{ ps}$ for $S/N > 14 - 35 - 70$

For a MIP in the 300 μm , 200 μm , 120 μm Sensors after 3'000fb⁻¹ expect

$S/N > 7 - 3 - 1.5 \Rightarrow 20\text{ps}$ for $\sim 5 - 10 - 20 \text{ MIPs}$

Appendix

Energy Resolution

Electromagnetic Calorimeters – Energy Resolution

Stochastic Term

Homogenous Calorimeter

- fluctuations of energy deposited in the active volume does not fluctuate event by event
- In most cases the intrinsic energy resolution can be better than the statistical expectation
- The correction factor is called Fano factor

$$\frac{\sigma_E}{E} = \frac{1}{\sqrt{E}}$$

Typical stochastic terms of homogeneous electromagnetic calorimeters are at the level of few percent

$$\frac{1}{\sqrt{E(\text{GeV})}}$$

- Energy resolution dominated by other effects

Sampling Calorimeters

- Energy deposited in active volume fluctuates because active layers are interleaved with absorber layers
- “sampling fluctuations” represent most important limitation to energy resolution of sampling calorimeters

Sampling term (Amaldi, 1981)

$$\frac{\sigma}{E} = \frac{1}{\sqrt{N_{ch}}} \propto \sqrt{\frac{t}{E_0(\text{GeV})}}$$

N_{ch} : number of charged particles crossing the active layer

T : thickness of absorber layers

smaller $t \Rightarrow$ larger sampling of shower by active layers \Rightarrow better energy resolution

Electromagnetic Calorimeters – Energy Resolution

Noise Term

Contribution from **electronic noise of the readout chain** and depends on the detector technique and on features of the readout circuit

Calorimeters in which the **signal is collected in the form of light** (scintillator-based sampling or homogenous calorimeters) can **achieve small levels of noise** if the first step of the electronic chain is a photosensitive device, like a PMT, which provides a **high-gain multiplication of the original signal with almost no noise**.

The noise is larger for detectors in which the signal is collected in the form of charge because the first element of the readout chain is a preamplifier

Noise can be minimized by signal shaping and optimal filtering to maximize the S/N ratio. However in general noise increases when operating at higher rates (larger amplifier bandwidth is required)

The noise equivalent energy is usually required to be much smaller than 100MeV per channel per applications in the several GeV region

Electromagnetic Calorimeters – Energy Resolution

Constant term

Not dependent on the particle energy

Instrumental effects that produce detector response non-uniformities: detector geometry, Imperfections in the mechanical structure and readout system, temperature gradients, aging, radiation damage, etc.

With the increasing energy of the present and future accelerators constant term becomes more and more the dominant contribution to the energy resolution \Rightarrow very tight requirements on construction tolerances

Typically the constant term should be kept at the level $\sim 1\%$ or smaller.

\Rightarrow This is particularly true for homogenous calorimeters, because of their smaller stochastic term.

Additional contributions to the noise

- Longitudinal leakage: energetic showers can lose part of their energy beyond the end of the active volume
- Lateral leakage: to limit electronic noise and pile-up \Rightarrow shower reconstructed in a relatively small cluster of cells
- Upstream energy losses: losses in the material preceding the calorimeter (other detectors, structures, cables, etc.)
- Non-hermetic coverage: cracks and dead regions